Discontinuous transition to a superconducting phase

Takumi Sato [1], Shingo Kobayashi [2], and Yasuhiro Asano [1]
[1] Department of Applied Physics, Hokkaido University, Sapporo 060-8628, Japan
[2] RIKEN Center for Emergent Matter Science, Wako, Saitama 351-0198, Japan

(Received 13 August 2023; revised 21 August 2024; accepted 23 August 2024; published 3 October 2024)

We discuss the instability of uniform superconducting states in $j = 3/2$ superconductors that contain the pairing correlations belonging to the odd-frequency symmetry class. The instability originates from the paramagnetic response of odd-frequency Cooper pairs and is considerable at finite temperatures. As a result, the pair potential varies discontinuously at the transition temperature when the amplitude of the odd-frequency pairing correlation functions is sufficiently large. We also discuss the discontinuous transition in other uniform superconductors.

DOI: 10.1103/PhysRevB.110.144503

I. INTRODUCTION

There are two types of uniform perturbations that act on uniform superconducting states. One does not change the thermal properties, while the other does. Spin-orbit interactions and Zeeman fields correspond to the examples of such perturbations in a spin-singlet superconductor. Spin-orbit interactions do not change any thermal properties of a superconductor such as the transition temperature T_c or the dependence of order parameter Δ on temperatures T [1]. On the other hand, uniform Zeeman fields decrease T_c. Moreover, the transition to the superconducting phase by decreasing the temperature changes to a first-order transition in sufficiently strong Zeeman fields [2,3]. Namely, the superconducting state is thermally unstable under Zeeman fields. A recent study [4] has reported that $j = 3/2$ superconductors also exhibit very similar instabilities. Although such discontinuous transition has been observed in spin-singlet superconductors under Zeeman fields [5–7], there has been no comprehensive explanation for why the superconducting transition changes to a first-order transition and what distinguishes the two types of perturbations. We address these issues in the present paper.

To the best of our knowledge, odd-frequency Cooper pairs [8–13] tend to cause thermal instability in superconducting states. This consideration is supported by the following findings for odd-frequency pairs localized various places in a superconductor such as at a vortex core [14], in the vicinity of a magnetic cluster [15,16], and at the surface of a topologically nontrivial superconductor [17,18]. An analysis of the free-energy density shows that the superconducting states are unstable locally around these defects [19,20]. The paramagnetic response of odd-frequency Cooper pairs to an external magnetic field is responsible for the instability [21]. In uniform superconductors, odd-frequency Cooper pairs exist as subdominant pairing correlations when the electronic structures have extra degrees of freedom such as spins, orbitals and sublattices [22]. It has been shown that the T_c of such superconductors decreases as the amplitude of odd-frequency pairs increases [23].

The purpose of this paper is to show that a uniform superconductor having a large amplitude of odd-frequency Cooper pairs exhibit the discontinuous transition from the normal state to the superconducting state. For this purpose, we analyze the way in which the odd-frequency pairing correlation functions change the coefficient of the Δ^4 term in the Ginzburg-Landau (GL) free-energy functional and the superfluid density. We find that the odd-frequency pairing correlations decrease the coefficient and the superfluid density in the same manner. The instability originates from the suppression of the superfluid density due to odd-frequency pairs. We conclude that the discontinuous transition to the superconducting phase is a common feature of superconductors that contain a large amount of uniform paramagnetic odd-frequency Cooper pairs in their superconducting phase. The two types of uniform perturbations are distinguished by whether they induce odd-frequency Cooper pairs.

This paper is organized as follows: In Sec. II, we explain a model of $j = 3/2$ superconductors which we mainly analyze in this paper and show the expression of the coefficients in the GL free-energy functional in terms of the Green's function. The discontinuous transition to the superconducting phase is demonstrated numerically in Sec. III. The mechanism of the discontinuous transition is discussed by analyzing the temperature dependence of the superfluid density in Sec. IV. In Sec. V, we discuss the discontinuous transition in other cases by analyzing a spin-singlet superconductor in Zeeman fields and a two-band superconductor under the band-hybridization. The conclusions are given in Sec. VI.

II. GINZBURG-LANDAU FREE ENERGY

A. Multiband superconductors

In this paper, we mainly analyze the Hamiltonian of pseudospin-quintet states in a $j = 3/2$ superconductor for the following several reasons. The normal-state Hamiltonian describes the most general multiband electronic states, which have four internal degrees of freedom and preserve both time-reversal symmetry and inversion symmetry [24]. The pair potential can be represented by a simple formula [25,26]. Useful mathematical tools are available to calculate the Green's function analytically. The high-pseudospin electronic states stem from the strong coupling between orbitals with angular momentum $\ell = 1$ and spin with $s = 1/2$ [25–29]. The mean-field Hamiltonian can be expressed as

$$\mathcal{H} = \frac{1}{2}\sum_{\boldsymbol{k}} \vec{\Psi}_{\boldsymbol{k}}^{\dagger} H(\boldsymbol{k}) \vec{\Psi}_{\boldsymbol{k}} + \frac{N\Delta^2}{\tilde{g}}, \quad (1)$$

$$\vec{\Psi}_{\boldsymbol{k}} = \left[\vec{\psi}_{\boldsymbol{k}}^{\mathrm{T}}, \vec{\psi}_{-\boldsymbol{k}}^{\dagger}\right]^{\mathrm{T}}, \quad (2)$$

$$\vec{\psi}_{\boldsymbol{k}} = [c_{\boldsymbol{k},3/2}, c_{\boldsymbol{k},1/2}, c_{\boldsymbol{k},-1/2}, c_{\boldsymbol{k},-3/2}]^{\mathrm{T}}, \quad (3)$$

where $\tilde{g} > 0$ represents the strength of the attractive interaction, N is the number of unit cells of the underlying lattice, Δ denotes the pair potential, and $c_{\boldsymbol{k},j_z}$ is the annihilation operator of an electron at $\boldsymbol{k}$ with pseudospin j_z. The Bogoliubov–de Gennes (BdG) Hamiltonian in Eq. (1) is

$$H(\boldsymbol{k}) = \begin{bmatrix} H_{\mathrm{N}}(\boldsymbol{k}) & \Delta(\boldsymbol{k}) \\ -\Delta^*(-\boldsymbol{k}) & -H_{\mathrm{N}}^*(-\boldsymbol{k}) \end{bmatrix}. \quad (4)$$

The normal-state Hamiltonian is represented by the tight-binding model on a simple cubic lattice [27] as

$$\begin{aligned} H_{\mathrm{N}}(\boldsymbol{k}) &= -2t_1 \sum_{\nu} \cos k_\nu - 2t_2 \sum_{\nu} \cos k_\nu J_\nu^2 \\ &\quad + 4t_3 \sum_{\nu \neq \nu'} \sin k_\nu \sin k_{\nu'} J_\nu J_{\nu'} + 6t_1 + \frac{15}{2}t_2 - \mu, \\ &= \xi_{\boldsymbol{k}} + \vec{\epsilon}_{\boldsymbol{k}} \cdot \vec{\gamma}, \end{aligned} \quad (5)$$

with μ being the chemical potential. The corresponding point group is O_h. The nearest-neighbor hopping independent of (depending on) pseudospin is t_1 (t_2). The second neighbor hopping is denoted by t_3. $\xi_{\boldsymbol{k}}$ represents kinetic energy of an electron and the five-component vector $\vec{\epsilon}_{\boldsymbol{k}}$ determines the dependence of the normal-state dispersions on pseudospins. The expressions of $\vec{\epsilon}_{\boldsymbol{k}}$ and five 4×4 matrices γ^{j} for j = 1–5 are given in Appendix A. The pair potential is represented by

$$\Delta(\boldsymbol{k}) = \Delta \vec{\eta}_{\boldsymbol{k}} \cdot \vec{\gamma} U_T, \quad (6)$$

$$\vec{\eta}_{\boldsymbol{k}} = (\eta_{\boldsymbol{k},1}, \eta_{\boldsymbol{k},2}, \eta_{\boldsymbol{k},3}, \eta_{\boldsymbol{k},4}, \eta_{\boldsymbol{k},5}), \quad (7)$$

where the five-component vector $\vec{\eta}_{\boldsymbol{k}}$ with $|\vec{\eta}_{\boldsymbol{k}}| = \sqrt{\vec{\eta}_{\boldsymbol{k}} \cdot \vec{\eta}_{\boldsymbol{k}}^*} = 1$ represents an even-parity pseudospin-quintet pairing order. The Fermi-Dirac statistics of electrons implies

$$\Delta^{\mathrm{T}}(-\boldsymbol{k}) = -\Delta(\boldsymbol{k}). \quad (8)$$

Here T means the transpose of the matrix which represents the interchange of pseudospins at two electrons in a Cooper pair. Since $[\vec{\eta}_{\boldsymbol{k}} \cdot \vec{\gamma} U_T]^{\mathrm{T}} = -\vec{\eta}_{\boldsymbol{k}} \cdot \vec{\gamma} U_T$, the pseudospin-quintet states are antisymmetric under interchanging two pseudospins.

B. Ginzburg-Landau expansion

To analyze superconducting states, we solve the Gor'kov equation

$$[i\omega_n - H(\boldsymbol{k})]\begin{bmatrix} \mathcal{G}(\boldsymbol{k}, i\omega_n) & \mathcal{F}(\boldsymbol{k}, i\omega_n) \\ -\underset{\sim}{\mathcal{F}}(\boldsymbol{k}, i\omega_n) & -\underset{\sim}{\mathcal{G}}(\boldsymbol{k}, i\omega_n) \end{bmatrix} = 1, \quad (9)$$

where $\omega_n = (2n+1)\pi T$ is the fermionic Matsubara frequency with n being an integer, and $\underset{\sim}{X}(\boldsymbol{k}, i\omega_n) \equiv X^*(-\boldsymbol{k}, i\omega_n)$ represents the particle-hole conjugation of $X(\boldsymbol{k}, i\omega_n)$. The anomalous Green's function satisfies $\mathcal{F}^{\mathrm{T}}(-\boldsymbol{k}, -i\omega_n) = -\mathcal{F}(\boldsymbol{k}, i\omega_n)$ due to the Fermi-Dirac statistics of electrons. The GL free-energy functional per unit cell is represented in terms of the Green's function [30,31]

$$\Omega_{\mathrm{SN}}(\Delta) = a\Delta^2 + b\Delta^4 + c\Delta^6 + \text{higher-order terms}, \quad (10)$$

$$a\Delta^2 = \frac{\Delta^2}{\tilde{g}} + T\sum_{\omega_n} \frac{1}{N}\sum_{\boldsymbol{k}} \frac{1}{2}\mathrm{Tr}[\mathcal{F}_1(\boldsymbol{k}, i\omega_n)\Delta^\dagger(\boldsymbol{k})], \quad (11)$$

$$b\Delta^4 = T\sum_{\omega_n} \frac{1}{N}\sum_{\boldsymbol{k}} \frac{1}{4}\mathrm{Tr}[\mathcal{F}_1(\boldsymbol{k}, i\omega_n)\Delta^\dagger(\boldsymbol{k})\mathcal{F}_1(\boldsymbol{k}, i\omega_n)\Delta^\dagger(\boldsymbol{k})], \quad (12)$$

where $\mathcal{F}_1(\boldsymbol{k}, i\omega_n) \equiv -\mathcal{G}_{\mathrm{N}}(\boldsymbol{k}, i\omega_n)\Delta(\boldsymbol{k})\underset{\sim}{\mathcal{G}}_{\mathrm{N}}(\boldsymbol{k}, i\omega_n)$ is the anomalous Green's function within the first order of Δ and $\mathcal{G}_{\mathrm{N}}(\boldsymbol{k}, i\omega_n) = [i\omega_n - H_{\mathrm{N}}(\boldsymbol{k})]^{-1}$ is the Green's function in the normal state. In a usual second-order transition, the equation $a = 0$ gives the transition temperature T_c. The inequalities $a < 0$ and $b > 0$ describe the stable superconducting state for $T < T_c$.

The anomalous Green's function for Eqs. (5) and (6) consists of four components as

$$\begin{aligned} \mathcal{F}_1(\boldsymbol{k}, i\omega_n) &= \frac{\Delta}{Z_0}\big[f_1^{\Delta}(\boldsymbol{k}, i\omega_n) + f_1^{\mathrm{s}}(\boldsymbol{k}, i\omega_n) + f_1^{\mathrm{q}}(\boldsymbol{k}, i\omega_n) \\ &\quad + f_1^{\mathrm{odd}}(\boldsymbol{k}, i\omega_n)\big], \end{aligned} \quad (13)$$

$$\begin{aligned} f_1^{\Delta}(\boldsymbol{k}, i\omega_n) &= -\left(\omega_n^2 + \xi_{\boldsymbol{k}}^2\right)\vec{\eta}_{\boldsymbol{k}} \cdot \vec{\gamma} U_T, \\ f_1^{\mathrm{s}}(\boldsymbol{k}, i\omega_n) &= 2\xi_{\boldsymbol{k}}\vec{\eta}_{\boldsymbol{k}} \cdot \vec{\epsilon}_{\boldsymbol{k}} U_T, \\ f_1^{\mathrm{q}}(\boldsymbol{k}, i\omega_n) &= -\vec{\epsilon}_{\boldsymbol{k}} \cdot \vec{\gamma}\vec{\eta}_{\boldsymbol{k}} \cdot \vec{\gamma}\vec{\epsilon}_{\boldsymbol{k}} \cdot \vec{\gamma} U_T, \end{aligned} \quad (14)$$

$$f_1^{\mathrm{odd}}(\boldsymbol{k}, i\omega_n) = -i\omega_n P_{\mathrm{O}} U_T, \quad P_{\mathrm{O}} = [\vec{\eta}_{\boldsymbol{k}} \cdot \vec{\gamma}, \vec{\epsilon}_{\boldsymbol{k}} \cdot \vec{\gamma}], \quad (15)$$

$$\begin{aligned} Z_0 &= \left(\omega_n^2 + \xi_{\boldsymbol{k}}^2 - \vec{\epsilon}_{\boldsymbol{k}}^{\,2}\right)^2 + 4\omega_n^2\vec{\epsilon}_{\boldsymbol{k}}^{\,2} \\ &= \xi_{\boldsymbol{k}}^4 + 2\xi_{\boldsymbol{k}}^2\left(\omega_n^2 - \vec{\epsilon}_{\boldsymbol{k}}^{\,2}\right) + \left(\omega_n^2 + \vec{\epsilon}_{\boldsymbol{k}}^{\,2}\right)^2, \end{aligned} \quad (16)$$

with $[A, B] = AB - BA$. f_1^{Δ} in Eq. (13) belongs to pseudospin-quintet symmetry and is linked to the pair potential through the gap equation. The spin-orbit interactions $\vec{\epsilon}_{\boldsymbol{k}}$ induce a pseudospin-singlet correlation function f_1^{s} and another pseudospin-quintet correlation function f_1^{q}. f_1^{odd} represents an induced pairing correlation belonging to the odd-frequency symmetry class and is finite for $P_{\mathrm{O}} \neq 0$ [32,33]. The structure of f_1^{q} is modified by f_1^{odd} because the two correlation functions are related to each other through the Gor'kov equation in Eq. (9). Therefore, the pseudospin-quintet components linked to the pair potential are indirectly modified by the odd-frequency component. The singlet component f_1^{s} and odd-frequency component f_1^{odd} do not form any pair potentials because the attractive interactions for the corresponding pairing channels are absent at the starting Hamiltonian.

In the absence of the odd-frequency pairing correlations (i.e., $P_{\mathrm{O}} = 0$), the coefficients in the free-energy functional are calculated to be

$$f_1^{\mathrm{q}}(\boldsymbol{k}, i\omega_n) = -\vec{\epsilon}_{\boldsymbol{k}}^{\,2}\vec{\eta}_{\boldsymbol{k}} \cdot \vec{\gamma} U_T, \tag{17}$$

$$a = \frac{1}{\tilde{g}} + T\sum_{\omega_n}\frac{1}{N}\sum_{\boldsymbol{k}}\frac{-2}{Z_0}\big(\omega_n^2 + \xi_{\boldsymbol{k}}^2 + \vec{\epsilon}_{\boldsymbol{k}}^{\,2}\big), \tag{18}$$

$$b = T\sum_{\omega_n}\frac{1}{N}\sum_{\boldsymbol{k}}\frac{1}{Z_0^2}\big\{\big(\omega_n^2 + \xi_{\boldsymbol{k}}^2 + \vec{\epsilon}_{\boldsymbol{k}}^{\,2}\big)^2 + 4\xi_{\boldsymbol{k}}^2\vec{\epsilon}_{\boldsymbol{k}}^{\,2}\big\} \times \{2 - |\vec{\eta}_{\boldsymbol{k}} \cdot \vec{\eta}_{\boldsymbol{k}}|^2\}. \tag{19}$$

$\vec{\epsilon}_{\boldsymbol{k}}^{\,2}$ in the last term of the numerator of Eq. (18) originates from f_1^{q} and amplifies the integrand. The gap equation corresponding to $a = 0$ has the same expression as that in the BCS theory [33]. In addition, the coefficient b is always positive. As a result, the transition to the superconducting state is second order and the superconducting state is stable for $T < T_c$. Therefore, the equation $P_{\mathrm{O}} = 0$ characterizes the perturbations that preserve the thermal properties of the superconducting states. Namely, the thermal properties of superconducting states in the absence of odd-frequency Cooper pairs are identical to those in the BCS state. We note that the thermal properties of a pseudospin-singlet superconducting state are also identical to those in the BCS state as shown in Appendix B.

In the presence of odd-frequency pairing correlation (i.e., $P_{\mathrm{O}} \neq 0$), it is not easy to obtain analytical expression of the GL coefficients without further simplifications. To proceed discussions, we restrict ourselves to consider E_g pairing order $\vec{\eta}_{\boldsymbol{k}} = (0, 0, 0, \eta_{\boldsymbol{k},4}, \eta_{\boldsymbol{k},5})$ because there are only two components in the pair potential. This simplification enables us to get the following analytical expressions:

$$f_1^{\mathrm{q}}(\boldsymbol{k}, i\omega_n) = \vec{\epsilon}_{\boldsymbol{k}}^{\,2}\vec{\eta}_{\boldsymbol{k}} \cdot \vec{\gamma} U_T - 2\vec{\epsilon}_{\boldsymbol{k}} \cdot \vec{\eta}_{\boldsymbol{k}}\vec{\epsilon}_{\boldsymbol{k}} \cdot \vec{\gamma} U_T, \tag{20}$$

$$a = \frac{1}{\tilde{g}} + T\sum_{\omega_n}\frac{1}{N}\sum_{\boldsymbol{k}}\frac{-2}{Z_0}\big(\omega_n^2 + \xi_{\boldsymbol{k}}^2 + \vec{\epsilon}_{\boldsymbol{k}}^{\,2} - 2A_0\big),$$

$$A_0 = \vec{\epsilon}_{\boldsymbol{k}}^{\,2} - |\vec{\epsilon}_{\boldsymbol{k}} \cdot \vec{\eta}_{\boldsymbol{k}}|^2, \tag{21}$$

$$\begin{aligned} b = T\sum_{\omega_n}\frac{1}{N}\sum_{\boldsymbol{k}}\frac{1}{Z_0^2}\Big[&\big(\omega_n^2 + \xi_{\boldsymbol{k}}^2 - \vec{\epsilon}_{\boldsymbol{k}}^{\,2}\big)^2 - 4\omega_n^2\vec{\epsilon}_{\boldsymbol{k}}^{\,2} \\ &- \big\{\big(\omega_n^2 + \xi_{\boldsymbol{k}}^2 - \vec{\epsilon}_{\boldsymbol{k}}^{\,2}\big)^2 - 4\omega_n^2\big(\epsilon_{\boldsymbol{k},1}^2 + \epsilon_{\boldsymbol{k},2}^2 + \epsilon_{\boldsymbol{k},3}^2 \\ &- \epsilon_{\boldsymbol{k},4}^2 - \epsilon_{\boldsymbol{k},5}^2\big)\big\}\eta_{\boldsymbol{k},4}^2(\eta_{\boldsymbol{k},5} - \eta_{\boldsymbol{k},5}^*)^2 \\ &+ 8|\vec{\epsilon}_{\boldsymbol{k}} \cdot \vec{\eta}_{\boldsymbol{k}}|^2\big(\omega_n^2 + \xi_{\boldsymbol{k}}^2 - \vec{\epsilon}_{\boldsymbol{k}}^{\,2} + |\vec{\epsilon}_{\boldsymbol{k}} \cdot \vec{\eta}_{\boldsymbol{k}}|^2\big)\Big], \end{aligned} \tag{22}$$

where we chose the common phase factor of the pair potential so that Δ and $\eta_{\boldsymbol{k},4}$ are real but $\eta_{\boldsymbol{k},5}$ is complex in general.

We found that the expression of f_1^{q} and a in Eqs. (20) and (21) is also valid for the general case: $\vec{\eta}_{\boldsymbol{k}} = (\eta_{\boldsymbol{k},1}, \eta_{\boldsymbol{k},2}, \eta_{\boldsymbol{k},3}, \eta_{\boldsymbol{k},4}, \eta_{\boldsymbol{k},5})$. Comparing with Eq. (17), the sign of the first term in Eq. (20) is reversed due to f_1^{odd} and a correction appears at the second term. Comparing with Eq. (18), an additional term $-2A_0$ appears in Eq. (21) to compensate for the presence of odd-frequency pairs. Since $A_0 \geqq 0$, the odd-frequency component f_1^{odd} suppresses the amplitudes of the pseudospin-quintet components, which leads to the suppression of T_c [23]. Similar arguments have also been presented in other papers [12,34,35]. The paramagnetic property of uniform odd-frequency Cooper pairs are summarized in Appendix C. Even under the simplifications in the pair potential $\vec{\eta}_{\boldsymbol{k}} = (0, 0, 0, \eta_{\boldsymbol{k},4}, \eta_{\boldsymbol{k},5})$, $P_{\mathrm{O}} \neq 0$ makes the expression of the coefficient b lengthy and complicated as shown in Eq. (22). To obtain the physical insights from the analytical expression of b, we consider specific examples such as $(\eta_{\boldsymbol{k},4}, \eta_{\boldsymbol{k},5}) = (1, 0)$, $(0, 1)$, $(1, 1)/\sqrt{2}$, and $(1, i)/\sqrt{2}$. The first, second, and fourth ones are predicted to be stable states within the phenomenological GL theory [26,28,36]. The commutator in Eq. (15) is calculated for (1,0) state

$$P_{\mathrm{O}}^{(1,0)} = 2\gamma^4\sum_{\mathrm{i}\neq 4}\epsilon_{\boldsymbol{k},\mathrm{i}}\gamma^{\mathrm{i}}. \tag{23}$$

The results for (0,1), $(1, 1)/\sqrt{2}$, and $(1, i)/\sqrt{2}$ states are given in Appendix D. The resulting correlation functions in Eq. (15) have a common matrix structure

$$f_1^{\mathrm{odd}}(\boldsymbol{k}, i\omega_n) \propto i\omega_n\sum_{\mathrm{i}=4,5}\sum_{\mathrm{j}\neq\mathrm{i}}a_{\mathrm{i,j}}(\boldsymbol{k})\gamma^{\mathrm{i}}\gamma^{\mathrm{j}}U_T, \tag{24}$$

where $a_{\mathrm{i,j}}$ is an even-parity function. Since $[f_1^{\mathrm{odd}}(\boldsymbol{k}, i\omega_n)]^{\mathrm{T}} = f_1^{\mathrm{odd}}(\boldsymbol{k}, i\omega_n)$, the induced odd-frequency pairing correlations consist of pseudospin-triplet states and pseudospin-septet states.

The expression of the coefficient b

$$b^{\mathrm{TRS}} = T\sum_{\omega_n}\frac{1}{N}\sum_{\boldsymbol{k}}\frac{1}{Z_0^2}\Big[\big(\omega_n^2 + \xi_{\boldsymbol{k}}^2 - \vec{\epsilon}_{\boldsymbol{k}}^{\,2}\big)^2 + 4|\vec{\epsilon}_{\boldsymbol{k}} \cdot \vec{\eta}_{\boldsymbol{k}}|^2\big(\omega_n^2 + 2\xi_{\boldsymbol{k}}^2 - 2A_0\big) - 4\omega_n^2A_0\Big], \tag{25}$$

is common in all the time-reversal invariant states $(\eta_{\boldsymbol{k},4}, \eta_{\boldsymbol{k},5}) = (1, 0)$, $(0, 1)$, and $(1, 1)/\sqrt{2}$. The results of b for a time-reversal breaking state $(1, i)/\sqrt{2}$ are given in Appendix D. The last terms proportional to ω_n^2 in Eqs. (25) and (D4) originate from f_1^{odd} and are always less than or equal to zero. Thus, the last term decreases the coefficient b down to zero when the amplitude of f_1^{odd} is sufficiently large. The relation $P_{\mathrm{O}} \neq 0$ in Eq. (15) characterizes perturbations that change the thermal properties of the superconducting states. Therefore, the two types of perturbations mentioned in the introduction are distinguished by whether they induce odd-frequency Cooper pairs.

The sixth- and higher-order terms in Eq. (10) are also modified by the odd-frequency correlation functions. However, it is not easy to separate the contributions of the odd-frequency correlations from those of the even-frequency correlations because of their cross terms. An example of the analytical expression of the sixth-order coefficient c is given in Appendix E.

III. DISCONTINUOUS TRANSITION

In this section, we demonstrate that the transition to the superconducting phase becomes discontinuous when the amplitude of the odd-frequency pairing components are sufficiently large. We choose $t_2 = 0$ in the normal-state Hamiltonian in Eq. (5). This simplification enables us to solve the Gor'kov equation in Eq. (9) analytically up to the infinite order of Δ. In what follows, we consider a pair potential $(\eta_{\boldsymbol{k},4}, \eta_{\boldsymbol{k},5}) = (1, 0)$ preserving time-reversal symmetry. The following discussions are valid also for $(\eta_{\boldsymbol{k},4}, \eta_{\boldsymbol{k},5}) =$

$(0, 1)$, $(1, 1)/\sqrt{2}$, and $(1, i)/\sqrt{2}$. We found that the thermal properties are the same among these states at $t_2 = 0$. The existence of odd-frequency Cooper pairs is a common feature among these states. The anomalous Green's function for $(\eta_{k,4}, \eta_{k,5}) = (1, 0)$ results in

$$\mathcal{F}(\boldsymbol{k}, i\omega_n) = -\frac{\Delta}{Z}[W - 2i\omega_n \vec{\epsilon}_{\boldsymbol{k}} \cdot \vec{\gamma}]\vec{\eta}_{\boldsymbol{k}} \cdot \vec{\gamma} U_T, \quad (26)$$

$$Z = W^2 + 4\omega_n^2 \vec{\epsilon}_{\boldsymbol{k}}^{\,2}, \quad W = \omega_n^2 + \xi_{\boldsymbol{k}}^2 - \vec{\epsilon}_{\boldsymbol{k}}^{\,2} + \Delta^2. \quad (27)$$

The second term in Eq. (26) is the pairing correlation belonging to the odd-frequency symmetry class, which is induced by the spin-orbit interaction $\vec{\epsilon}_{\boldsymbol{k}}$. The coefficient of the fourth-order term is calculated to be

$$b(T) = T \sum_{\omega_n} \frac{1}{N} \sum_{\boldsymbol{k}} \frac{1}{Z_0^2}\left[W_0^2 - 4\omega_n^2 \vec{\epsilon}_{\boldsymbol{k}}^{\,2}\right], \quad (28)$$

with $Z_0 = Z|_{\Delta=0}$ and $W_0 = W|_{\Delta=0}$. The last term in Eq. (28) is derived from the odd-frequency pairing correlation functions and contributes negatively to the coefficient b as already mentioned in Eq. (25). The amplitude of the pair potential Δ is determined self-consistently from the thermodynamic potential in the superconducting state

$$\Omega_{\mathrm{S}}(\Delta) = \frac{\Delta^2}{\tilde{g}} - \frac{2T}{N} \sum_{\boldsymbol{k}, \lambda = \mathrm{S}\pm} \ln\left[2\cosh\left(\frac{E_\lambda(\boldsymbol{k})}{2T}\right)\right], \quad (29)$$

where $E_{\mathrm{S}\pm}(\boldsymbol{k}) = \sqrt{\xi_{\boldsymbol{k}}^2 + \Delta^2} \pm |\vec{\epsilon}_{\boldsymbol{k}}|$ and irrelevant constants are neglected. The pair potential is determined by minimizing $\Omega_{\mathrm{S}}(\Delta)$ with respect to Δ. Thus, the solution in the equilibrium state (Δ_{eq}) always satisfies

$$\Omega_{\mathrm{SN}}(\Delta_{\mathrm{eq}}) = \min_{\Delta}\{\Omega_{\mathrm{SN}}(\Delta) | \Delta \in \mathbb{R}\} \leqq 0, \quad (30)$$

with $\Omega_{\mathrm{SN}}(\Delta) \equiv \Omega_{\mathrm{S}}(\Delta) - \Omega_{\mathrm{S}}(0)$. The solution of Δ_{eq} is plotted as a function of temperature in Fig. 1(a) for several choices of spin-orbit interaction t_3. Hereafter, the transition temperature at $t_3 = 0$ is denoted by T_0, and the pair potential at $T = 0$ and $t_3 = 0$ is denoted by Δ_0. In the numerical simulation, we chose $\mu = t_1$ and $\tilde{g} = 2.463t_1$ so that $T_0 = 0.05t_1$. We obtained $\Delta_0 = 0.0882t_1 \approx 1.76T_0$, which corresponds to BCS universal relation [37]. The transition temperature decreases monotonically with increasing t_3. Although Δ_{eq} is insensitive to t_3 at very low temperature $T \ll T_0$, it abruptly vanishes for $t_3 \gtrsim 0.023t_1$. Uniform superconducting states are no longer stable under strong spin-orbit couplings. Furthermore, Δ_{eq} shows the discontinuous behavior at T_c for $t_3 \gtrsim 0.0205t_1$. In Fig. 1(b), the coefficient $b(T_c)$ is plotted as a function of t_3. We obtained $b(T_0) = 1.237t_1^{-3}$ at $t_3 = 0$. As predicted in Eq. (28), the odd-frequency pairing correlations decrease the coefficient $b(T_c)$. As a result, the transition becomes discontinuous for $b(T_c) < 0$ as shown in Figs. 1(a) and 1(b). Thus, odd-frequency Cooper pairs are responsible for the discontinuous transition to the superconducting states.

IV. SUPERFLUID DENSITY

To understand why odd-frequency Cooper pairs cause the discontinuous transition, we discuss the relationship between the coefficient b and the response function to an electromagnetic field,

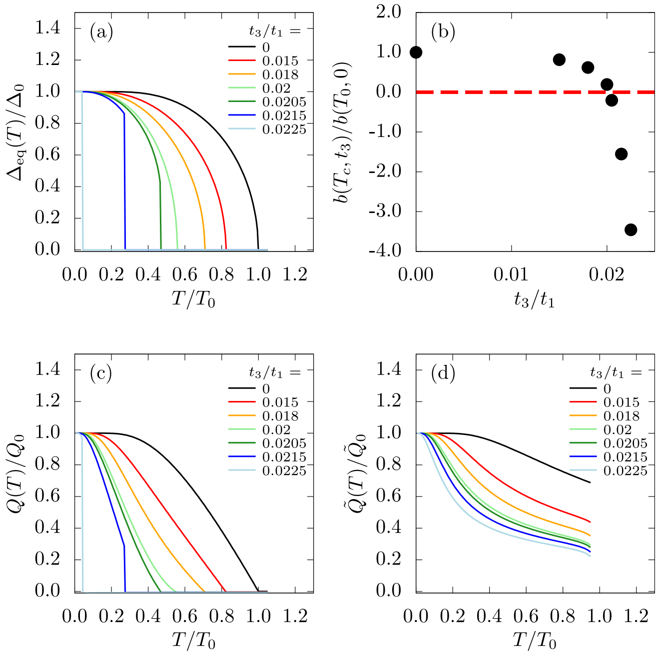

FIG. 1. The self-consistent solution of the pair potential $\Delta_{\mathrm{eq}}(T)$ in a $j = 3/2$ superconductor is plotted as a function of temperature for several strengths of spin-orbit interaction t_3 in panel (a), where T_0 is the transition temperature at $t_3 = 0$ and Δ_0 is the amplitude of the pair potential at $T = 0$ and $t_3 = 0$. The coefficient b at $T = T_c$ is plotted as a function of t_3 in panel (b), where T_c is obtained from the results in panel (a). The temperature dependence of the superfluid density Q and $\tilde{Q}$ is shown in panels (c) and (d), respectively. Q_0 ($\tilde{Q}_0$) in panel (c) [(d)] represents Q ($\tilde{Q}$) at $T = 0$ and $t_3 = 0$.

$$j_x(\boldsymbol{q}, \omega) = -K_{xx}(\boldsymbol{q}, \omega)A_x(\boldsymbol{q}, \omega), \quad (31)$$

where j_ν is the electric current and $A_\nu(\boldsymbol{q}, \omega)$ is the Fourier component of a vector potential. The derivation of the response kernel $K_{\nu\nu}$ is presented in Appendix F. The response kernel to a static transverse gauge potential is called Meissner kernel or *superfluid density*:

$$Q = \frac{K_{xx}(\boldsymbol{q} \to 0, \omega = 0)}{2e^2 t_1}, \quad (32)$$

where e is the charge of an electron and Q has no dimensions. In Fig. 1(c), the superfluid density Q is plotted as a function of temperature for several choices of t_3, where $Q_0 = 0.0664$ is the superfluid density at $T = 0$ and $t_3 = 0$ in our numerical simulation. At $T \approx 0$, the superfluid density is almost independent of t_3 for $t_3 \lesssim 0.0225t_1$. However, the superfluid density decreases drastically at finite temperatures. To understand such characteristic features, we analyze the contribution of the anomalous Green's function in Eq. (26) to the superfluid density,

$$Q^{\mathcal{F}} = T \sum_{\omega_n} \frac{1}{N} \sum_{\boldsymbol{k}} 2t_1 \sin^2 k_x \frac{4\Delta^2}{Z^2}\left[W^2 - 4\omega_n^2 \vec{\epsilon}_{\boldsymbol{k}}^{\,2}\right]. \quad (33)$$

The second term is derived from the odd-frequency pairing correlations and reduces the superfluid density. The dependence of Q on temperature in Fig. 1(c) is dominated mainly by that of $\Delta_{\rm eq}^2(T)$ because Q is proportional to $\Delta_{\rm eq}^2(T)$ as shown in Eq. (33). Thus, it is not easy to extract the effects of odd-frequency pairs on the superfluid density. To highlight a role of odd-frequency pairs in the discontinuous transition, we calculate.

$$\tilde{Q}(T, t_3) = \frac{Q(T, t_3, \Delta_{\rm BCS}(T))}{\Delta_{\rm BCS}^2(T)}, \tag{34}$$

for $T < T_0$. Here we first replace $\Delta_{\rm eq}(T, t_3)$ by

$$\Delta_{\rm BCS}(T) = \Delta_{\rm eq}(T, t_3 = 0) \tag{35}$$

and divide the results by $\Delta_{\rm BCS}^2(T)$ to relax the influence of $\Delta_{\rm BCS}(T)$. In Fig. 1(d), $\tilde{Q}$ is plotted for several choices of t_3. The vertical axis is normalized to $\tilde{Q}_0 = \tilde{Q}(T = 0, t_3 = 0)$. The black line for $t_3 = 0$ almost corresponds to the results of BCS theory

$$\frac{\tilde{Q}(T, t_3 = 0)}{\tilde{Q}_0} \approx \Delta_0^2 \pi T \sum_{\omega_n} \frac{1}{\left[\omega_n^2 + \Delta_{\rm BCS}^2(T)\right]^{3/2}}, \tag{36}$$

and decreases with increasing temperature almost linearly for $T \gtrsim 0.3T_0$. $\tilde{Q}$ at $T = 0$ remains unchanged even in the presence of the spin-orbit interaction, whereas it at finite temperatures decreases with increasing t_3. The suppression from the black line is remarkable for $0.2 \lesssim T/T_0 \lesssim 0.5$. As a result, the curves for $t_3/t_1 = 0.015$–0.0225 are convex downward. The drastic suppression of the superfluid density in such finite temperatures is responsible for the suppression of T_c and the discontinuous transition finding at $t_3/t_1 \gtrsim 0.0205$.

When we compare Eq. (28) with Eq. (33), the odd-frequency pairs decrease the coefficient b and the superfluid density $Q^{\mathcal{F}}$ in the same manner. The two values are related to each other by the relation

$$b \approx A Q^{\mathcal{F}}/\Delta^2|_{\Delta\to 0}, \tag{37}$$

with $A > 0$ being a constant. $Q^{\mathcal{F}}$ in Eq. (37) would be replaced by Q (total superfluid density) if we can perform the momentum integration analytically. The relationship between b and Q in Eq. (37) at the discontinuous transition is a central finding in this paper. We revisit the relation in other superconducting states in Sec. V. As shown in Eq. (26), the odd-frequency pairing correlation function is proportional to the Matsubara frequency, which is a common property of odd-frequency pairs in uniform superconductors [12,23]. As a result, the instability due to odd-frequency pairs is considerable at finite temperatures [38]. We conclude that the discontinuous transition to the superconducting phase occurs because odd-frequency Cooper pairs reduce the superfluid density at finite temperatures.

V. DISCONTINUOUS TRANSITION IN OTHER CASES

A. Other $j = 3/2$ states

The discontinuous transition due to odd-frequency Cooper pairs and the relationship in Eq. (37) are confirmed in other superconducting states. Indeed, the expression in Eqs. (28) and (33) can be applied also to other E_g states such as $(\eta_{\boldsymbol{k},4}, \eta_{\boldsymbol{k},5}) = (0, 1)$ and $(1, 1)/\sqrt{2}$ at $t_2 = 0$.

The discontinuous transition in $j = 3/2$ superconductors has also been reported in T_{2g} pairing states at $T \geqq 0$ [4]. The authors of Ref. [4] concluded that the interband pair potentials are responsible for the discontinuous transition. Here, *band* means the diagonalized normal-state band (i.e., Bloch band). The pair potentials for such T_{2g} states can be described as

$$\vec{\eta}_{\boldsymbol{k}} = (0, \eta_{\boldsymbol{k},2}, \eta_{\boldsymbol{k},3}, 0, 0). \tag{38}$$

The odd-frequency Cooper pairs exist also in T_{2g} states. Since the commutator in Eq. (15) for T_{2g} states is calculated to be

$$P_{\rm O}^{T_{2g}} = 2\left(\eta_{\boldsymbol{k},2}\gamma^2 \sum_{\rm i\neq 2} \epsilon_{\boldsymbol{k},\rm i}\gamma^{\rm i} + \eta_{\boldsymbol{k},3}\gamma^3 \sum_{\rm i\neq 3} \epsilon_{\boldsymbol{k},\rm i}\gamma^{\rm i}\right), \tag{39}$$

the odd-frequency pairing correlation function has a mathematical structure of

$$f_1^{\rm odd}(\boldsymbol{k}, i\omega_n) \propto i\omega_n \sum_{\rm i=2,3} \sum_{\rm j\neq i} a_{\rm i,j}(\boldsymbol{k})\gamma^{\rm i}\gamma^{\rm j} U_T. \tag{40}$$

The correlation function has essentially the same structures as that in Eq. (24). Such an analysis suggests that the discontinuous transition due to odd-frequency Cooper pairs also occurs in the T_{2g} states. Unfortunately, however, we cannot conclude clearly because we cannot derive the relation in Eq. (37) analytically.

In Ref. [4], the authors pointed out an important role of interband pair potentials in the discontinuous transition. Thus it seems meaningful to compare the two pairing states and sort out their relationship. The interband pair potential and odd-frequency pairing are not equivalent concept to each other. To make this point clear, we consider a two-band superconductor described by

$$H_{\rm BdG}(\boldsymbol{k}) = \begin{bmatrix} E_{\rm N}(\boldsymbol{k}) & \Delta(\boldsymbol{k}) \\ \Delta(\boldsymbol{k}) & -E_{\rm N}(\boldsymbol{k}) \end{bmatrix}, \tag{41}$$

$$E_{\rm N} = \begin{bmatrix} \epsilon_1 & 0 \\ 0 & \epsilon_2 \end{bmatrix}, \quad \Delta = \begin{bmatrix} \Delta_1 & 0 \\ 0 & \Delta_2 \end{bmatrix}, \tag{42}$$

where the normal-state Hamiltonian is diagonalized by a unitary transformation. We assume that the pair potential has only diagonal elements in the Bloch band picture. The spin symmetry and the momentum-parity of the pair potentials Δ_j can be either spin-singlet even parity or spin-triplet odd parity. We assume $E_{\rm N}(-\boldsymbol{k}) = E_{\rm N}(\boldsymbol{k})$ for simplicity. The BdG Hamiltonian can be block-diagonalized for each band. Therefore, the interband pair potentials are absent in such a superconducting state. The odd-frequency pairing correlation in this case $f^{\rm odd} \propto i\omega_n[E_{\rm N}\Delta - \Delta E_{\rm N}]$ is also absent because the commutator is zero. Next, we introduce the interband superconducting order parameter

$$\Delta = \begin{bmatrix} \Delta_1 & \Delta_{12} \\ \Delta_{12} & \Delta_2 \end{bmatrix}. \tag{43}$$

Here we assume that Δ_{12} appears as a results of the unitary transformation that diagonalizes the normal state Hamiltonian. Three pairing correlations contribute to the pair potential in Eq. (43). In addition to the two intraband pairing correlations, the interband pairing correlation forms the pair potentials. The pair potential in Eq. (43) satisfies $\Delta^{\rm T} = \Delta$, which means the pair potentials are symmetric under interchanging the band indices. When the two bands are identical to each other $\epsilon_1 = \epsilon_2$, $E_{\rm N}$ is proportional to the identity matrix and commutes with Δ. As a result, the odd-frequency pairing correlation is absent. For $\epsilon_1 \neq \epsilon_2$, the asymmetry between the two bands generates the odd-frequency pairs as a subdominant pairing correlation

$$f_{\text{odd}} \propto i\omega_n \begin{bmatrix} 0 & \Delta_{12}(\epsilon_1 - \epsilon_2) \\ -\Delta_{12}(\epsilon_1 - \epsilon_2) & 0 \end{bmatrix}. \tag{44}$$

In contrast with the interband pairing correlation forming Δ_{12} in Eq. (43), the induced interband pairing correlation is antisymmetric under interchanging band indices, (i.e., $f^{\text{T}}_{\text{odd}} = -f_{\text{odd}}$). Cooper pairs linked to Δ_{12} belong to even-frequency even-band-parity symmetry class, whereas induced Cooper pairs belong to odd-frequency odd-band-parity symmetry class. Such symmetry conversion occurs because the band asymmetry preserves both spin configurations and momentum parity of a Cooper pair. Thus, the interband pair potential and the odd-frequency Cooper pairing are different concepts from each other. In Ref. [4], the authors may not distinguish two interband Cooper pairs. However, in this paper, we clearly distinguish the two interband pairs because they contribute to the superfluid density in opposite ways to each other.

The instability at $T = 0$ for both T_{2g} and E_g pairing states has been also discussed in Ref. [39]. The authors of Ref. [39] compared the free energy among multiple superconducting states with changing the amplitude of the attractive interaction between the two electrons. They found that the transition to another superconducting phase becomes first-order. Odd-frequency pairing correlations are also present in these superconducting states. Therefore, the transition from the normal state to one of these superconducting states would be discontinuous when the amplitude of the odd-frequency pairs are sufficiently large.

B. Other $s = 1/2$ states

In addition to $j = 3/2$ superconductors, the discontinuous transition has been found in other superconducting states of $s = 1/2$ electrons. The transition in a two-band superconductor with interband pairing order becomes one of the examples when the band hybridization V is sufficiently large [40]. We note that *bands* in Ref. [40] indicates atomic orbitals rather than the Bloch bands. In this model, the band-hybridization corresponds to the perturbation which generates odd-frequency Cooper pairs. The paramagnetic property of the odd-frequency Cooper pairs explains well the mechanism of the discontinuous transition. The analysis for such an interband superconductor in Ref. [40] is presented in Appendix G. We also discuss the effects of band asymmetry ϵ on the discontinuous transition. The fourth-order coefficient of the GL free energy b and the superfluid density Q share the same expression as shown in Eq. (G6). As a result, we confirm the relation in Eq. (37) also in a two-band superconductor.

Finally, we emphasize the relevance of the conclusions in this paper to an important open issue. The transition to the uniform spin-singlet s-wave superconducting state is known to be discontinuous under a Zeeman field B [2,3,41,42]. The calculated results for the coefficient b and the superfluid density Q are given by

$$b = \frac{N_0}{4} Y(A_0, C_0), \tag{45}$$

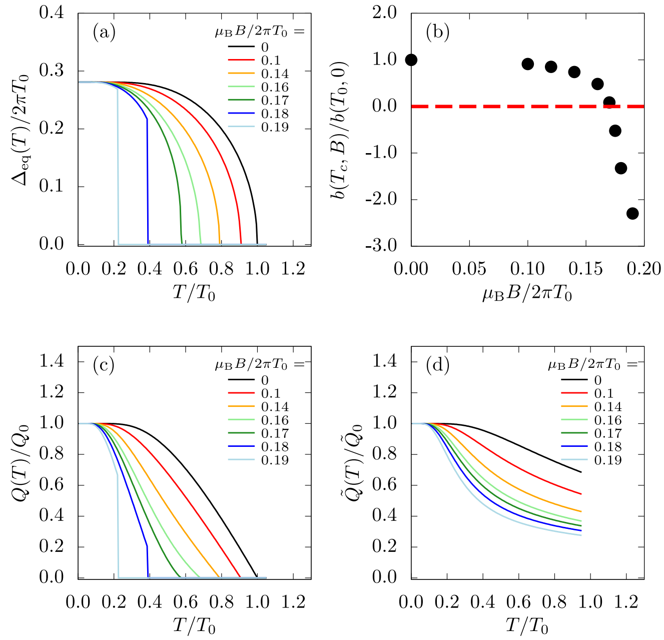

FIG. 2. The self-consistent solution of the pair potential $\Delta_{\text{eq}}(T)$ in a spin-singlet superconductor under a Zeeman field is plotted as a function of temperature for several strengths of Zeeman interaction B in panel (a), where T_0 is the transition temperature at $B = 0$ and Δ_0 is the amplitude of the pair potential at $T = 0$ and $B = 0$. The coefficient b at $T = T_c$ is plotted as a function of B in panel (b), where T_c is obtained from the results in panel (a). The temperature dependence of the superfluid density Q and $\tilde{Q}$ is shown in panels (c) and (d), respectively. Q_0 ($\tilde{Q}_0$) in panel (c) [(d)] represents Q ($\tilde{Q}$) at $T = 0$ and $B = 0$.

$$Q = 2n\Delta^2 Y(A, C), \tag{46}$$

$$Y(A, C) = \sqrt{2}\pi T \sum_{\omega_n} \frac{A^3 + \sqrt{C}\left(A^2 - 2\omega_n^2 \mu_{\text{B}}^2 B^2\right)}{[C(A + \sqrt{C})]^{3/2}}, \tag{47}$$

$$A = \Delta^2 + \omega_n^2 - \mu_{\text{B}}^2 B^2, \quad C = A^2 + 4\omega_n^2 \mu_{\text{B}}^2 B^2, \tag{48}$$

with $A_0 = A|_{\Delta=0}$ and $C_0 = C|_{\Delta=0}$, where N_0 is the density of states at the Fermi level per spin in the normal state, n is the electron density per spin, and μ_{B} is Bohr's magneton. The derivations are given in Appendix H. We also calculate

$$\tilde{Q}(T, B) = \frac{Q(T, B, \Delta_{\text{BCS}}(T))}{\Delta^2_{\text{BCS}}(T)} = 2nY(A, C)|_{\Delta=\Delta_{\text{BCS}}(T)}, \tag{49}$$

where $\Delta_{\text{BCS}}(T) = \Delta_{\text{eq}}(T, B = 0)$ represents the pair potential of a BCS superconductor. The last term in Eq. (47) is derived from the odd-frequency pairing correlation, which is generated by a Zeeman field. The coefficient b and the superfluid density Q satisfy the relation in Eq. (37). The self-consistent pair potential Δ_{eq}, the coefficient b at the transition temperature, the superfluid density Q, and $\tilde{Q}$ in the spin-singlet superconductor are plotted in Figs. 2(a)–2(d), respectively. We denote the transition temperature at $B = 0$ by T_0 and the pair potential at $T = 0$ and $B = 0$ by $\Delta_0 \approx 1.76T_0$ [37]. The coefficient b at $T = T_0$ and $B = 0$ corresponds to the BCS

TABLE I. Three theoretical models which describe the discontinuous transition to the superconducting phase. The structures of the pair potential are given in the second row. The third row shows the perturbations that induce odd-frequency pairing correlations. The transition to the superconducting state becomes discontinuous because odd-frequency Cooper pairs decrease the superfluid density to zero. The fourth-order coefficient of the GL free energy b and the superfluid density Q are proportional to each other, as shown in Eq. (37).

	$j = 3/2$ SC	Conventional SC	Two-band SC
Pair potential	$\Delta\vec{\eta}_k \cdot \vec{\gamma} U_T$	$\Delta i\hat{\sigma}_2$	$\Delta i\hat{\rho}_2$
Perturbation	Spin-orbit interaction $\vec{\epsilon}_k \cdot \vec{\gamma}$	Zeeman field $\mu_B \boldsymbol{B} \cdot \hat{\boldsymbol{\sigma}}$[a]	Band hybridization and asymmetry $\varepsilon\hat{\rho}_3 + V\hat{\rho}_1$[b]
$b \approx AQ^{(\mathcal{F})}/\Delta^2\|_{\Delta\to 0}$	Eqs. (28) and (33)	Eqs. (45) and (46)	Eq. (G6)

[a] $\hat{\sigma}_j$ for j = 1–3 are Pauli matrices in spin space.
[b] $\hat{\rho}_j$ for j = 1–3 are Pauli matrices in band space.

results:

$$b_{BCS}(T_0) = N_0 \frac{7\zeta(3)}{16(\pi T_0)^2}. \quad (50)$$

$Q_0 = 2n$ is the superfluid density at $T = 0$ and $B = 0$. $\tilde{Q}_0 = 2n/\Delta_0^2$ represents $\tilde{Q}$ at $T = 0$ and $B = 0$. The characteristic properties shown in Fig. 2 are almost identical to those in Fig. 1.

In Table I, we summarize the obtained results for three theoretical models of superconducting state. The second row shows the structure of the pair potentials. The third row shows the perturbations that generate the odd-frequency pairing correlations. Since $f^{\text{odd}} \propto i\omega_n[H_N(\boldsymbol{k})\Delta(\boldsymbol{k}) - \Delta(\boldsymbol{k})\underset{\sim}{H}_N(\boldsymbol{k})]$, it is easy to confirm the presence of odd-frequency pairs when the normal-state Hamiltonian H_N includes the perturbations on the table. Although these three models describe different superconducting states in different electronic structures, the coefficient b and the superfluid density Q share essentially the same expression as shown in Eq. (37). The existence of odd-frequency Cooper pairs is a common feature among the three uniform superconducting states. The discontinuous transition occurs because odd-frequency Cooper pairs decrease the superfluid density at finite temperature. The results displayed on Table I suggest that the origin of the phenomenon among these models is common. In this paper, we find a sufficient condition that makes the transition to the superconducting phase discontinuous. We do not deny other mechanisms for the discontinuous transition.

C. A relating state

The Fulde-Ferrell-Larkin-Ovchinnikov (FFLO) state is expected at high Zeeman fields [43,44]. For $\mu_B B/2\pi T_0 \gtrsim 0.18$, such spatially oscillating states can be a stable solution of the Gor'kov equation [45]. Theoretical studies [46,47] showed that the transition from the normal state to the FFLO state can be both first and second order depending on model parameters. Since odd-frequency Cooper pairs also exist in such regime [48,49], there might be nontrivial relationships between the nonuniform odd-frequency Cooper pairs and the order of the phase transition. However, the problem is beyond the scope of this paper and is left for our future study.

VI. CONCLUSION

We have theoretically studied the thermodynamic instability of uniform superconducting states that include the subdominant pairing correlations belonging to the odd-frequency symmetry class. We especially focus on roles of odd-frequency Cooper pairs in the discontinuous transition to the superconducting phase. In $j = 3/2$ superconductors, we analyzed the contributions of the odd-frequency pairing correlations to the coefficient of Δ^4 term in the Ginzburg-Landau (GL) free energy b and the superfluid density Q. The odd-frequency pairing correlations decrease b and Q down to zero in the same manner because odd-frequency Cooper pairs are paramagnetic. Since the effects are considerable at finite temperatures, the transition to a superconducting phase becomes discontinuous. At a low temperature far below the transition temperature, on the other hand, the pair potential and the superfluid density remain unchanged even in the presence of odd-frequency pairs. The dependence of the odd-frequency pairing correlation functions on the Matsubara frequency explains well such characteristic features of the instability.

We also analyze the discontinuous transition in other superconductors such as a conventional s-wave spin-singlet superconductor under Zeeman fields and a two-band superconductor with interband pairing order. If odd-frequency Cooper pairs significantly reduce the superfluid density, the transitions to these superconducting states can be discontinuous. The coefficient b and the superfluid density Q calculated for these states also share essentially the same expressions. We conclude that the discontinuous transition to the uniform superconducting state is a common feature of superconductors in which the amplitude of the odd-frequency pairing correlation function is sufficiently large.

ACKNOWLEDGMENTS

The authors are grateful to A. A. Golubov, Y. Tanaka, Y. V. Fominov, and S. Hoshino for useful discussions. T.S. was supported by JST, the establishment of university fellowships towards the creation of science technology innovation, Grant No. JPMJFS2101. S.K. was supported by JSPS KAKENHI (Grants No. JP19K14612 and No. JP22K03478) and JST CREST (Grant No. JPMJCR19T2).

APPENDIX A: ALGEBRAS OF γ MATRICES

The dispersions in the normal-state Hamiltonian are given by

$$\xi_{\boldsymbol{k}} = \left(-2t_1 - \frac{5}{2}t_2\right)\sum_{\nu}\cos k_\nu + 6t_1 + \frac{15}{2}t_2 - \mu, \tag{A1}$$

$$\epsilon_{\boldsymbol{k},1} = 4\sqrt{3}t_3 \sin k_x \sin k_y, \tag{A2}$$

$$\epsilon_{\boldsymbol{k},2} = 4\sqrt{3}t_3 \sin k_y \sin k_z, \tag{A3}$$

$$\epsilon_{\boldsymbol{k},3} = 4\sqrt{3}t_3 \sin k_z \sin k_x, \tag{A4}$$

$$\epsilon_{\boldsymbol{k},4} = \sqrt{3}t_2(-\cos k_x + \cos k_y), \tag{A5}$$

$$\epsilon_{\boldsymbol{k},5} = t_2(-2\cos k_z + \cos k_x + \cos k_y). \tag{A6}$$

The spinors for the angular momentum of $j = 3/2$ are described by

$$J_x = \frac{1}{2}\begin{bmatrix} 0 & \sqrt{3} & 0 & 0 \\ \sqrt{3} & 0 & 2 & 0 \\ 0 & 2 & 0 & \sqrt{3} \\ 0 & 0 & \sqrt{3} & 0 \end{bmatrix}, \tag{A7}$$

$$J_y = \frac{1}{2}\begin{bmatrix} 0 & -i\sqrt{3} & 0 & 0 \\ i\sqrt{3} & 0 & -2i & 0 \\ 0 & 2i & 0 & -i\sqrt{3} \\ 0 & 0 & i\sqrt{3} & 0 \end{bmatrix}, \tag{A8}$$

$$J_z = \frac{1}{2}\begin{bmatrix} 3 & 0 & 0 & 0 \\ 0 & 1 & 0 & 0 \\ 0 & 0 & -1 & 0 \\ 0 & 0 & 0 & -3 \end{bmatrix}. \tag{A9}$$

The five Dirac's γ-matrices are defined in 4×4 pseudospin space as

$$\gamma^1 = \tfrac{1}{\sqrt{3}}(J_xJ_y + J_yJ_x), \quad \gamma^2 = \tfrac{1}{\sqrt{3}}(J_yJ_z + J_zJ_y), \tag{A10}$$

$$\gamma^3 = \tfrac{1}{\sqrt{3}}(J_zJ_x + J_xJ_z), \quad \gamma^4 = \tfrac{1}{\sqrt{3}}\left(J_x^2 - J_y^2\right), \tag{A11}$$

$$\gamma^5 = \frac{1}{3}\left(2J_z^2 - J_x^2 - J_y^2\right), \tag{A12}$$

and $1_{4\times4}$ is the identity matrix. They satisfy the following relations:

$$\gamma^{\mathrm{i}}\gamma^{\mathrm{j}} + \gamma^{\mathrm{j}}\gamma^{\mathrm{i}} = 2 \times 1_{4\times4}\delta_{\mathrm{i,j}}, \tag{A13}$$

$$\gamma^1\gamma^2\gamma^3\gamma^4\gamma^5 = -1_{4\times4}, \tag{A14}$$

$$\{\gamma^{\mathrm{i}}\}^* = \{\gamma^{\mathrm{i}}\}^{\mathrm{T}} = U_T\gamma^{\mathrm{i}}U_T^{-1}, \quad U_T = \gamma^1\gamma^2, \tag{A15}$$

where U_T is the unitary part of the time-reversal operation $\mathcal{T} = U_T\mathcal{K}$ with $\mathcal{K}$ meaning complex conjugation. Equation (5) corresponds to the Luttinger-Kohn Hamiltonian [27] with cubic anisotropy when we expand the trigonometric functions up to the second order of the momentum.

APPENDIX B: PSEUDOSPIN-SINGLET PAIRING ORDER

Pseudospin-singlet pair potential in the $j = 3/2$ model is described by

$$\Delta(\boldsymbol{k}) = \Delta U_T, \tag{B1}$$

in the BdG Hamiltonian in Eq. (4) [25,26]. Here, Δ is chosen to be real. The anomalous Green's function within the first order of Δ results in

$$\mathcal{F}_1^{\mathrm{singlet}} = \frac{\Delta}{Z_0}\left[-\left(\omega_n^2 + \xi_{\boldsymbol{k}}^2 + \vec{\epsilon}_{\boldsymbol{k}}^{\,2}\right) + 2\xi_{\boldsymbol{k}}\vec{\epsilon}_{\boldsymbol{k}}\cdot\vec{\gamma}\right]U_T. \tag{B2}$$

In this pairing order, the spin-orbit interaction does not induce any odd-frequency pairing correlations but generates an even-frequency pseudospin-quintet pairing correlation described by the second term in Eq. (B2). The coefficients in the GL free-energy functional are expressed as

$$a^{\mathrm{singlet}} = \frac{1}{\tilde{g}} + T\sum_{\omega_n}\frac{1}{N}\sum_{\boldsymbol{k}}\frac{-2}{Z_0}\left(\omega_n^2 + \xi_{\boldsymbol{k}}^2 + \vec{\epsilon}_{\boldsymbol{k}}^{\,2}\right), \tag{B3}$$

$$b^{\mathrm{singlet}} = T\sum_{\omega_n}\frac{1}{N}\sum_{\boldsymbol{k}}\frac{1}{Z_0^2}\left\{\left(\omega_n^2 + \xi_{\boldsymbol{k}}^2 + \vec{\epsilon}_{\boldsymbol{k}}^{\,2}\right)^2 + 4\xi_{\boldsymbol{k}}^2\vec{\epsilon}_{\boldsymbol{k}}^{\,2}\right\}, \tag{B4}$$

where a^{singlet} and b^{singlet} represent second- and fourth-order coefficients of the GL functional, respectively. The expression of a^{singlet} is equivalent to a in Eq. (18) and $b^{\mathrm{singlet}} > 0$ holds true. Therefore, the thermal property of the pseudospin-singlet state is identical to that of the BCS state as well as the pseudospin-quintet states without odd-frequency Cooper pairs discussed in Sec. II B.

APPENDIX C: PARAMAGNETIC PROPERTY OF ODD-FREQUENCY COOPER PAIR

We consider a general Bogoliubov–de Gennes Hamiltonian describing electronic states of a uniform superconductor:

$$H(\boldsymbol{k}) = \begin{bmatrix} H_{\mathrm{N}}(\boldsymbol{k}) & \Delta(\boldsymbol{k}) \\ -\utilde{\Delta}(\boldsymbol{k}) & -\utilde{H}_{\mathrm{N}}(\boldsymbol{k}) \end{bmatrix}, \tag{C1}$$

where $\utilde{X}(\boldsymbol{k}, i\omega_n) = X^*(-\boldsymbol{k}, i\omega_n)$ represents particle-hole conjugation. We assume $H(\boldsymbol{k})$ is a $2M \times 2M$ matrix with M being a positive integer. $H(\boldsymbol{k})$ has particle-hole symmetry described as

$$CH(-\boldsymbol{k})C^{-1} = -H(\boldsymbol{k}), \quad C = \tau_1\mathcal{K}, \tag{C2}$$

where C represents charge-conjugation operator and τ_j for $j = 1$–3 are Pauli matrices in the particle-hole space. When we examine a response of superconductors to external perturbations within the linear response theory, we often need to compute a correlation function of this form:

$$\Pi = T\sum_{\omega_n}\frac{1}{V_{\rm vol}}\sum_{\boldsymbol{k}} A^2 \mathrm{Tr}[\mathcal{G}\underset{\sim}{\mathcal{G}} - \underset{\sim}{\mathcal{F}}\mathcal{F}]_{(\boldsymbol{k},i\omega_n)}, \tag{C3}$$

where A represents a vertex in a corresponding correlation function (e.g., current operator in a current-current correlation function) and $\mathcal{G}(\mathcal{F})$ is normal (anomalous) Green's function. The Green's function is calculated by the Gor'kov equation,

$$[i\omega_n - H(\boldsymbol{k})]\begin{bmatrix}\mathcal{G} & \mathcal{F}\\ -\underset{\sim}{\mathcal{F}} & -\underset{\sim}{\mathcal{G}}\end{bmatrix}_{(\boldsymbol{k},i\omega_n)} = 1. \tag{C4}$$

The relation

$$\mathcal{F}^{\rm T}(-\boldsymbol{k},-i\omega_n) = -\mathcal{F}(\boldsymbol{k},i\omega_n), \tag{C5}$$

holds true by the Fermi-Dirac statistics of electrons. The contribution of the anomalous Green's function to the correlation function is calculated to be

$$\begin{aligned}\Pi^{\mathcal{F}} &= T\sum_{\omega_n}\frac{1}{V_{\rm vol}}\sum_{\boldsymbol{k}} A^2\mathrm{Tr}[-\underset{\sim}{\mathcal{F}}(\boldsymbol{k},i\omega_n)\mathcal{F}(\boldsymbol{k},i\omega_n)]\\ &= T\sum_{\omega_n}\frac{1}{V_{\rm vol}}\sum_{\boldsymbol{k}} A^2\sum_{\alpha\beta}\mathcal{F}^*_{\beta\alpha}(\boldsymbol{k},-i\omega_n)\mathcal{F}_{\beta\alpha}(\boldsymbol{k},i\omega_n)\\ &= T\sum_{\omega_n}\frac{1}{V_{\rm vol}}\sum_{\boldsymbol{k}}\\ &\quad\times A^2\sum_{\alpha\beta}\left(\left|f^{\rm e}_{\beta\alpha}(\boldsymbol{k},i\omega_n)\right|^2 - \left|f^{\rm o}_{\beta\alpha}(\boldsymbol{k},i\omega_n)\right|^2\right),\end{aligned} \tag{C6}$$

where we used the relation in Eq. (C5) to reach the second line. $\mathcal{F}_{\beta\alpha}$ represents (β,α) component of the $M\times M$ matrix $\mathcal{F}$ and

$$f^{\rm e/o}_{\beta\alpha}(\boldsymbol{k},i\omega_n) = \frac{\mathcal{F}_{\beta\alpha}(\boldsymbol{k},i\omega_n) \pm \mathcal{F}_{\beta\alpha}(\boldsymbol{k},-i\omega_n)}{2} \tag{C7}$$

represents even- and odd-frequency components of $\mathcal{F}_{\beta\alpha}$. Equation (C6) clearly shows the anomalous properties of odd-frequency Cooper pairs by the negative sign of the second term. When we consider a linear response to a static transverse vector potential, the second term indicates that odd-frequency pairing correlations always have negative contributions to the Meissner kernel. In other words, odd-frequency Cooper pairs exhibit a paramagnetic response to external magnetic fields and then destabilize superconductivity by disturbing phase coherence. Actually, above arguments are not valid when the corresponding vertex cannot be factorized like Eq. (C3). It has been shown that diamagnetic odd-frequency Cooper pairs can exist in some special systems [50,51]. But the odd-frequency Cooper pairs in most multiband or orbital superconductors show paramagnetic response [23] and those considered in this paper are also paramagnetic.

APPENDIX D: INDUCED PAIRING CORRELATIONS

The odd-frequency pairing correlations induced by the spin-orbit interactions are represented by $f^{\rm odd}_1(\boldsymbol{k},i\omega_n) = -i\omega_n P_{\rm O} U_T$. We supply the calculated results of $P_{\rm O}$ for $(\eta_{\boldsymbol{k},4},\eta_{\boldsymbol{k},5}) = (0,1), (1,1)/\sqrt{2}$ and $(1,i)/\sqrt{2}$,

$$P^{(0,1)}_{\rm O} = 2\gamma^5\sum_{\rm i\neq 5}\epsilon_{\boldsymbol{k},\rm i}\gamma^{\rm i}, \tag{D1}$$

$$P^{(1,1)/\sqrt{2}}_{\rm O} = \sqrt{2}\Bigg[(\gamma^4+\gamma^5)\sum_{\rm i=1}^{3}\epsilon_{\boldsymbol{k},\rm i}\gamma^{\rm i} + (\epsilon_{\boldsymbol{k},5}-\epsilon_{\boldsymbol{k},4})\gamma^4\gamma^5\Bigg], \tag{D2}$$

$$P^{(1,i)/\sqrt{2}}_{\rm O} = \sqrt{2}\Bigg[(\gamma^4+i\gamma^5)\sum_{\rm i=1}^{3}\epsilon_{\boldsymbol{k},\rm i}\gamma^{\rm i} + (\epsilon_{\boldsymbol{k},5}-i\epsilon_{\boldsymbol{k},4})\gamma^4\gamma^5\Bigg]. \tag{D3}$$

The expression of the coefficient b for $(1,i)/\sqrt{2}$ state is given by

$$b^{\rm TRSB} = T\sum_{\omega_n}\frac{1}{N}\sum_{\boldsymbol{k}}\frac{1}{Z_0^2}\Big[2\big(\omega_n^2+\xi_{\boldsymbol{k}}^2-A_0 + |\vec{\epsilon}_{\boldsymbol{k}}\cdot\vec{\eta}_{\boldsymbol{k}}|^2\big)^2 - 8\omega_n^2(A_0-|\vec{\epsilon}_{\boldsymbol{k}}\cdot\vec{\eta}_{\boldsymbol{k}}|^2)\Big]. \tag{D4}$$

APPENDIX E: SIXTH-ORDER COEFFICIENT

The sixth-order coefficient of the GL functional in Eq. (10) is represented as

$$c\Delta^6 = T\sum_{\omega_n}\frac{1}{N}\sum_{\boldsymbol{k}}\frac{1}{6}\mathrm{Tr}[\mathcal{F}_1(\boldsymbol{k},i\omega_n)\Delta^\dagger(\boldsymbol{k}) \times\mathcal{F}_1(\boldsymbol{k},i\omega_n)\Delta^\dagger(\boldsymbol{k})\mathcal{F}_1(\boldsymbol{k},i\omega_n)\Delta^\dagger(\boldsymbol{k})]. \tag{E1}$$

When we choose $(\eta_{\boldsymbol{k},4},\eta_{\boldsymbol{k},5}) = (1,0)$ and $t_2 = 0$ in Eq. (4) as we assumed in Sec. III, the sixth-order coefficient of the GL functional results in

$$c = T\sum_{\omega_n}\frac{1}{N}\sum_{\boldsymbol{k}}\frac{-2}{3Z_0^3}\Big\{\big(\omega_n^2+\xi_{\boldsymbol{k}}^2-\vec{\epsilon}_{\boldsymbol{k}}^{\,2}\big)^3 - 12\omega_n^2\vec{\epsilon}_{\boldsymbol{k}}^{\,2}\big(\omega_n^2+\xi_{\boldsymbol{k}}^2-\vec{\epsilon}_{\boldsymbol{k}}^{\,2}\big)\Big\}. \tag{E2}$$

The first term in Eq. (E2) originates from the even-frequency correlation function. On the other hand, the second term is composed of both even and odd-frequency correlation function. Although eighth-order coefficients and above are also modified by odd-frequency correlation functions, it is difficult to extract the physical meaning from these coefficients due to the cross terms.

APPENDIX F: LINEAR RESPONSE TO ELECTROMAGNETIC FIELDS IN A LATTICE MODEL

The coupling between an electron and an electromagnetic field is considered through the Peierls phase in the kinetic energy [52,53]:

$$\mathcal{H}_{\rm N}^{\rm kin} = -t_1 \sum_{j_z} \sum_{\langle \boldsymbol{r}_{\rm i}, \boldsymbol{r}_{\rm j}\rangle} e^{i\varphi_{\rm ij}} c^\dagger_{\boldsymbol{r}_{\rm i}, j_z} c_{\boldsymbol{r}_{\rm j}, j_z} + \text{H.c.},$$

$$\varphi_{\rm ij} = e\int_{\boldsymbol{r}_{\rm j}}^{\boldsymbol{r}_{\rm i}} d\boldsymbol{r}\cdot \boldsymbol{A}(\boldsymbol{r}), \tag{F1}$$

where $c^\dagger_{\boldsymbol{r}, j_z}$ ($c_{\boldsymbol{r}, j_z}$) is the creation (annihilation) operator for the electron at $\boldsymbol{r}$ with pseudospin j_z. We neglect the correction to the weak spin-orbit interactions ($t_3 \ll t_1$). The current density operator $\boldsymbol{j}$ is defined from the variation of the Hamiltonian with respect to the vector potential:

$$\delta\mathcal{H}(t) = -\sum_{\boldsymbol{r}} \boldsymbol{j}(\boldsymbol{r}, t)\cdot \delta\boldsymbol{A}(\boldsymbol{r}, t). \tag{F2}$$

Within the first order of the vector potential, the current can be decomposed into the paramagnetic and diamagnetic terms,

$$j_\mu(\boldsymbol{r}, t) = j_\mu^{\rm para}(\boldsymbol{r}) + j_\mu^{\rm dia}(\boldsymbol{r}, t)\ (\mu = x,\ y,\ z), \tag{F3}$$

$$j_\mu^{\rm para}(\boldsymbol{r}) = iet_1\sum_{j_z}\left[c^\dagger_{\boldsymbol{r}+\hat{\boldsymbol{r}}_\mu, j_z} c_{\boldsymbol{r}, j_z} - \text{H.c.}\right],$$

$$j_\mu^{\rm dia}(\boldsymbol{r}, t) = e^2 k_\mu(\boldsymbol{r}) A_\mu(\boldsymbol{r}, t), \tag{F4}$$

where $\hat{\boldsymbol{r}}_\mu$ is the basic lattice vector along the μ direction of a simple cubic lattice and $k_\mu(\boldsymbol{r})$ is local kinetic-energy operator with respect to the μ-oriented links, which is defined as

$$k_\mu(\boldsymbol{r}) = -t_1\sum_{j_z}\left[c^\dagger_{\boldsymbol{r}+\hat{\boldsymbol{r}}_\mu, j_z} c_{\boldsymbol{r}, j_z} + \text{H.c.}\right]. \tag{F5}$$

The perturbation Hamiltonian $\mathcal{H}'$ within the first order of the vector potential reads

$$\mathcal{H}'(t) = -\sum_{\boldsymbol{r}} \boldsymbol{j}^{\rm para}(\boldsymbol{r})\cdot \boldsymbol{A}(\boldsymbol{r}, t). \tag{F6}$$

In Sec. IV, we examine the linear response in the x-direction:

$$j_x(\boldsymbol{q}, \omega) = -K_{xx}(\boldsymbol{q}, \omega) A_x(\boldsymbol{q}, \omega). \tag{F7}$$

The response kernel K_{xx} is calculated to be [54–56]

$$K_{xx}(\boldsymbol{q}, \omega) = e^2\langle -k_x(\boldsymbol{r})\rangle - \Lambda^{\rm R}_{xx}(\boldsymbol{q}, \omega), \tag{F8}$$

where $\langle -k_x(\boldsymbol{r})\rangle$ represents the kinetic energy along the x direction per unit cell and $\Lambda^{\rm R}_{xx}$ is the current-current correlation function expressed as

$$\Lambda^{\rm R}_{xx}(\boldsymbol{q}, \omega) = \Lambda_{xx}(\boldsymbol{q}, i\nu_m \to \omega + i\delta), \tag{F9}$$

$$\begin{aligned}\Lambda_{xx}(\boldsymbol{q}, i\nu_m) = -e^2 T\sum_{\omega_n}\frac{1}{N}\sum_{\boldsymbol{k}} 4t_1^2 \sin^2 k_x &\times \text{Tr}[\mathcal{G}(\boldsymbol{k}+\boldsymbol{q}, i\omega_n + i\nu_m)\mathcal{G}(\boldsymbol{k}, i\omega_n) \\ &- \underset{\sim}{\mathcal{F}}(\boldsymbol{k}+\boldsymbol{q}, i\omega_n + i\nu_m)\mathcal{F}(\boldsymbol{k}, i\omega_n)],\end{aligned} \tag{F10}$$

where $\nu_m = 2m\pi T$ is a bosonic Matsubara frequency with m being an integer and δ is a small positive real value. We only consider the transverse gauge fields [i.e., $\boldsymbol{q}\cdot \boldsymbol{A}(\boldsymbol{q}, \omega) = 0$]. The superfluid density is defined by

$$Q = \frac{K_{xx}(\boldsymbol{q}\to 0, \omega = 0)}{2e^2 t_1}. \tag{F11}$$

The contribution of odd-frequency pairing correlations in Sec. IV is described by using

$$Q^{\mathcal{F}} = T\sum_{\omega_n}\frac{1}{N}\sum_{\boldsymbol{k}} 2t_1\sin^2 k_x \text{Tr}[-\underset{\sim}{\mathcal{F}}(\boldsymbol{k}, i\omega_n)\mathcal{F}(\boldsymbol{k}, i\omega_n)]. \tag{F12}$$

The summation over Matsubara frequencies can be carried out analytically, when we use the spectral representation of the Green's function,

$$G(\boldsymbol{k}, i\omega_n) = \sum_\lambda \frac{\vec{\phi}_{\boldsymbol{k},\lambda}\vec{\phi}^\dagger_{\boldsymbol{k},\lambda}}{i\omega_n - E_\lambda(\boldsymbol{k})}. \tag{F13}$$

Here, the summation is taken over all eight indices of the eigenstates of the BdG Hamiltonian and $\vec{\phi}_{\boldsymbol{k},\lambda}$ is the eigenvector belonging to the eigenenergy $E_\lambda(\boldsymbol{k})$. After the summation over the Matsubara frequencies, we reach

$$\langle -k_x(\boldsymbol{r})\rangle = \frac{1}{N}\sum_{\boldsymbol{k},\lambda={\rm S}\pm} 2t_1\cos k_x\left[u_{\boldsymbol{k}}^2 f(E_\lambda) + v_{\boldsymbol{k}}^2 f(-E_\lambda)\right], \tag{F14}$$

with

$$u_{\boldsymbol{k}}^2 = 1 + \frac{\xi_{\boldsymbol{k}}}{\sqrt{\xi_{\boldsymbol{k}}^2 + \Delta^2}},\quad v_{\boldsymbol{k}}^2 = 1 - \frac{\xi_{\boldsymbol{k}}}{\sqrt{\xi_{\boldsymbol{k}}^2 + \Delta^2}}, \tag{F15}$$

and

$$\Lambda^{\rm R}_{xx}(\boldsymbol{q}\to 0, \omega = 0) = e^2\frac{1}{N}\sum_{\boldsymbol{k},\lambda={\rm S}\pm} 8t_1^2\sin^2 k_x\left(-\frac{\partial f(E_\lambda)}{\partial E_\lambda}\right), \tag{F16}$$

where $f(E) = [e^{E/T} + 1]^{-1}$ is Fermi distribution function. Above expressions are valid for $(\eta_{\boldsymbol{k},4}, \eta_{\boldsymbol{k},5}) = (1, 0)$, $(0, 1)$, and $(1, 1)/\sqrt{2}$ at $t_2 = 0$.

The Green's function for $(\eta_{\boldsymbol{k},4}, \eta_{\boldsymbol{k},5}) = (1, 0)$, $(0, 1)$, and $(1, 1)/\sqrt{2}$ at $t_2 = 0$ is calculated to be

$$\begin{aligned}\mathcal{G}(\boldsymbol{k}, i\omega_n) = -\frac{1}{Z}\big[&\left(\omega_n^2 + \xi_{\boldsymbol{k}}^2 + \Delta^2\right)(i\omega_n + \xi_{\boldsymbol{k}}) + \vec{\epsilon}_{\boldsymbol{k}}^{\,2}(i\omega_n - \xi_{\boldsymbol{k}}) \\ &- \left\{(i\omega_n + \xi_{\boldsymbol{k}})^2 + \Delta^2 - \vec{\epsilon}_{\boldsymbol{k}}^{\,2}\right\}\vec{\epsilon}_{\boldsymbol{k}}\cdot\vec{\gamma}\big],\end{aligned} \tag{F17}$$

$$\mathcal{F}(\boldsymbol{k}, i\omega_n) = -\frac{\Delta}{Z}\left[\omega_n^2 + \xi_{\boldsymbol{k}}^2 + \Delta^2 - \vec{\epsilon}_{\boldsymbol{k}}^{\,2} - 2i\omega_n\vec{\epsilon}_{\boldsymbol{k}}\cdot\vec{\gamma}\right]\vec{\eta}_{\boldsymbol{k}}\cdot\vec{\gamma}\, U_T, \tag{F18}$$

$$Z = \left(\omega_n^2 + \xi_{\boldsymbol{k}}^2 + \Delta^2 - \vec{\epsilon}_{\boldsymbol{k}}^{\,2}\right)^2 + 4\omega_n^2\vec{\epsilon}_{\boldsymbol{k}}^{\,2}. \tag{F19}$$

The last term in Eq. (F18) represents the odd-frequency pairing correlation induced by the spin-orbit interaction.

APPENDIX G: DISCONTINUOUS TRANSITION IN A TWO-BAND SUPERCONDUCTOR WITH INTERBAND PAIRING ORDER

We consider following mean-field Hamiltonian which describes the two-band superconducting states with the interband pairing order,

$$\mathcal{H} = \sum_{\boldsymbol{k}} [a^\dagger_{\boldsymbol{k},\uparrow}\ a^\dagger_{\boldsymbol{k},\downarrow}\ b^\dagger_{\boldsymbol{k},\uparrow}\ b^\dagger_{\boldsymbol{k},\downarrow} a_{-\boldsymbol{k},\uparrow}\ a_{-\boldsymbol{k},\downarrow}\ b_{-\boldsymbol{k},\uparrow}\ b_{-\boldsymbol{k},\downarrow}] \left[\begin{array}{cccc|cccc} \varepsilon^{\rm a}_{\boldsymbol{k}} & & V & & & & & \Delta \\ & \varepsilon^{\rm a}_{\boldsymbol{k}} & & V & & & s\Delta & \\ V & & \varepsilon^{\rm b}_{\boldsymbol{k}} & & & -s\Delta & & \\ & V & & \varepsilon^{\rm b}_{\boldsymbol{k}} & -\Delta & & & \\ \hline & & & -\Delta & -\varepsilon^{\rm a}_{\boldsymbol{k}} & & -V & \\ & & -s\Delta & & & -\varepsilon^{\rm a}_{\boldsymbol{k}} & & -V \\ & s\Delta & & & -V & & -\varepsilon^{\rm b}_{\boldsymbol{k}} & \\ \Delta & & & & & -V & & -\varepsilon^{\rm b}_{\boldsymbol{k}} \end{array}\right] \begin{bmatrix} a_{\boldsymbol{k},\uparrow} \\ a_{\boldsymbol{k},\downarrow} \\ b_{\boldsymbol{k},\uparrow} \\ b_{\boldsymbol{k},\downarrow} \\ a^\dagger_{-\boldsymbol{k},\uparrow} \\ a^\dagger_{-\boldsymbol{k},\downarrow} \\ b^\dagger_{-\boldsymbol{k},\uparrow} \\ b^\dagger_{-\boldsymbol{k},\downarrow} \end{bmatrix}, \tag{G1}$$

where $a^\dagger_{k\sigma}$ ($b^\dagger_{k\sigma}$) is a creation operator of an electron in band a (b) with momentum $\boldsymbol{k}$ and spin $\sigma (=\uparrow, \downarrow)$. $\varepsilon^{\rm l}_{\boldsymbol{k}}$ (l = a, b) is defined by $\varepsilon^{\rm l}_{\boldsymbol{k}} = \boldsymbol{k}^2/2m_{\rm l} - \mu_{\rm l}$ and V is the hybridization potential mixing the two bands. Δ represents interband pairing potential belonging to s-wave spin-triplet odd-band-parity (spin-singlet even-band-parity) symmetry class when we choose $s = +1$ (-1). Equation (G1) with $s = +1$ corresponds to the mean-field Hamiltonian considered in Ref. [40]. Equation (G1) can be block-diagonalized and the reduced 4×4 Hamiltonian is represented by

$$\check{H}(\boldsymbol{k}) = \begin{bmatrix} \hat{H}_{\rm N} & \hat{\Delta} \\ \hat{\Delta}^\dagger & -\hat{H}_{\rm N} \end{bmatrix}, \quad \hat{H}_{\rm N} = \xi + \varepsilon\hat{\rho}_3 + V\hat{\rho}_1, \quad \hat{\Delta} = \begin{cases} \Delta(i\hat{\rho}_2) & (s=+1) \\ \Delta\hat{\rho}_1 & (s=-1), \end{cases} \tag{G2}$$

where $\xi = (\varepsilon^{\rm a}_{\boldsymbol{k}} + \varepsilon^{\rm b}_{\boldsymbol{k}})/2$, $\varepsilon = (\varepsilon^{\rm a}_{\boldsymbol{k}} - \varepsilon^{\rm b}_{\boldsymbol{k}})/2$, and $\hat{\rho}_{\rm j}$ for j = 1–3 are Pauli matrices in the two-band space. The anomalous Green's function $\hat{\mathcal{F}}$ is calculated as

$$\hat{\mathcal{F}}(\boldsymbol{k}, i\omega_n) = \begin{cases} \frac{-1}{Z_{+1}}\left[\omega_n^2 + \xi^2 - \varepsilon^2 - V^2 + \Delta^2 - 2i\omega_n(\varepsilon\hat{\rho}_3 + V\hat{\rho}_1)\right]\Delta(i\hat{\rho}_2) & (s=+1) \\ \frac{-1}{Z_{-1}}\left[\omega_n^2 + \xi^2 - \varepsilon^2 + V^2 + \Delta^2 - 2V\xi\hat{\rho}_1 + 2iV\varepsilon\hat{\rho}_2 - 2i\omega_n\varepsilon\hat{\rho}_3\right]\Delta\hat{\rho}_1 & (s=-1), \end{cases} \tag{G3}$$

$$Z_{+1} = \left(\omega_n^2 + \xi^2 - \varepsilon^2 - V^2 + \Delta^2\right)^2 + 4\omega_n^2(\varepsilon^2 + V^2), \tag{G4}$$

$$Z_{-1} = \left(\omega_n^2 + \xi^2 - \varepsilon^2 + V^2 + \Delta^2\right)^2 - 4\left(V^2\xi^2 - V^2\varepsilon^2 - \omega_n^2\varepsilon^2\right). \tag{G5}$$

$-2i\omega_n\varepsilon\hat{\rho}_3\Delta(i\hat{\rho}_2)$ and $-2i\omega_n V\hat{\rho}_1\Delta(i\hat{\rho}_2)$ in the numerator for $s = +1$ and $-2i\omega_n\varepsilon\hat{\rho}_3\Delta\hat{\rho}_1$ in that for $s = -1$ represent odd-frequency pairing correlations.

The authors of Ref. [40] analyzed the transition from the normal state to the superconducting state described by $\mathcal{H}$ in Eq. (G1) with $s = +1$. They found that the transition becomes first-order under the sufficiently large band hybridization V. The mechanism is explained well by the paramagnetic property of the odd-frequency Cooper pairs induced by V as well as we discussed in this paper. Moreover, the discontinuous transition is also expected in the presence of sufficiently large asymmetry between the two bands ε. In this case, the odd-frequency pairing correlation is induced also by the band asymmetry ε. This argument is valid because $\check{H}(\boldsymbol{k})$ in Eq. (G2) for $s = +1$ is equivalent to the Hamiltonian of a spin-singlet superconductor under Zeeman fields. The calculated results of the fourth-order coefficient of the GL free energy and the superfluid density are given by

$$b \propto Y_{\rm inter}(A_0, C_0), \quad Q \propto \Delta^2 Y_{\rm inter}(A, C), \tag{G6}$$

with $Y_{\rm inter} = Y|_{\mu_{\rm B}B \to \sqrt{(\varepsilon^2+V^2)}}$ in Eq. (47). Here we consider a simple band structure $m_{\rm a} = m_{\rm b}$ [23] for simplicity.

APPENDIX H: A SPIN-SINGLET SUPERCONDUCTOR UNDER SPIN-DEPENDENT POTENTIALS

We consider a spatially uniform spin-singlet s-wave superconducting state under spin-dependent potentials. The Gor'kov equation reads

$$[i\omega_n - \check{H}_{\rm BdG}]\begin{bmatrix} \mathcal{G} & \mathcal{F} \\ -\underset{\sim}{\mathcal{F}} & -\underset{\sim}{\mathcal{G}} \end{bmatrix}_{(\boldsymbol{k}, i\omega_n)} = \check{1}, \quad \check{H}_{\rm BdG} = \begin{bmatrix} \hat{H}_{\rm N} & \hat{\Delta} \\ -\underset{\sim}{\hat{\Delta}} & -\underset{\sim}{\hat{H}}_{\rm N} \end{bmatrix}. \tag{H1}$$

The anomalous Green's function is represented as

$$\mathcal{F}(\boldsymbol{k}, i\omega_n) = \left[\hat{\Delta}\underset{\sim}{\hat{\Delta}} - \omega_n^2 - \hat{\Delta}\underset{\sim}{\hat{H}}_{\rm N}\hat{\Delta}^{-1}\hat{H}_{\rm N} + i\omega_n P\right]^{-1}\hat{\Delta}, \tag{H2}$$

$$P = \left(\hat{\Delta}\underset{\sim}{\hat{H}}_{\rm N} - \hat{H}_{\rm N}\hat{\Delta}\right)\hat{\Delta}^{-1}, \quad \hat{\Delta} = \Delta i\hat{\sigma}_2, \tag{H3}$$

where $\hat{\sigma}_{\rm j}$ for j = 1–3 are Pauli matrices in the spin space. The odd-frequency pairing correlations appear for $P \neq 0$ [12]. The electric current $\boldsymbol{j}$ within the linear response to a vector potential $\boldsymbol{A}$ is described by [57]

$$\boldsymbol{j} = -\frac{e^2}{mc} Q\boldsymbol{A},$$
$$Q = nT \sum_{\omega_n} \int d\xi \, \langle {\rm Tr}[\mathcal{G}\mathcal{G} - \underset{\sim}{\mathcal{F}}\mathcal{F} - \mathcal{G}_{\rm N}\mathcal{G}_{\rm N}]_{(\boldsymbol{k}, i\omega_n)} \rangle_{\rm FS}, \tag{H4}$$

where n is the electron density per spin, $\langle \cdots \rangle_{\rm FS} \equiv \int \frac{d\Omega}{4\pi} \cdots$ is the Fermi-surface average, and Q is referred to as superfluid density.

First, we consider the normal-state Hamiltonian including an antisymmetric spin-orbit interaction,

$$\hat{H}_{\rm N}(\boldsymbol{k}) = \xi_{\boldsymbol{k}} - \boldsymbol{\alpha}_{\boldsymbol{k}} \cdot \hat{\boldsymbol{\sigma}}, \quad \xi_{\boldsymbol{k}} = \frac{\hbar^2 \boldsymbol{k}^2}{2m} - \mu, \quad \boldsymbol{\alpha}_{-\boldsymbol{k}} = -\boldsymbol{\alpha}_{\boldsymbol{k}}. \tag{H5}$$

The Fermi surface is split into two due to the spin-orbit interaction in the normal state. The Green's functions are calculated to be

$$\mathcal{G}(\boldsymbol{k}, i\omega_n) = -\frac{(i\omega_n + \xi_{\boldsymbol{k}})(\omega_n^2 + \xi_{\boldsymbol{k}}^2 + \Delta^2) + (i\omega_n - \xi_{\boldsymbol{k}})\boldsymbol{\alpha}_{\boldsymbol{k}}^2 + \{(i\omega_n + \xi_{\boldsymbol{k}})^2 - \boldsymbol{\alpha}_{\boldsymbol{k}}^2 - \Delta^2\}\boldsymbol{\alpha}_{\boldsymbol{k}} \cdot \hat{\boldsymbol{\sigma}}}{\{\omega_n^2 + \xi_{\boldsymbol{k}}^2 + \Delta^2 + \boldsymbol{\alpha}_{\boldsymbol{k}}^2\}^2 - 4\xi_{\boldsymbol{k}}^2 \boldsymbol{\alpha}_{\boldsymbol{k}}^2}, \tag{H6}$$
$$\mathcal{F}(\boldsymbol{k}, i\omega_n) = -\frac{\omega_n^2 + \xi_{\boldsymbol{k}}^2 + \Delta^2 + \boldsymbol{\alpha}_{\boldsymbol{k}}^2 + 2\xi_{\boldsymbol{k}}\boldsymbol{\alpha}_{\boldsymbol{k}} \cdot \hat{\boldsymbol{\sigma}}}{\{\omega_n^2 + \xi_{\boldsymbol{k}}^2 + \Delta^2 + \boldsymbol{\alpha}_{\boldsymbol{k}}^2\}^2 - 4\xi_{\boldsymbol{k}}^2 \boldsymbol{\alpha}_{\boldsymbol{k}}^2} \Delta i\hat{\sigma}_2. \tag{H7}$$

The last term in the numerator of $\mathcal{F}$ represents the spin-triplet odd-parity pairing correlation induced by the spin-orbit interaction. Since $P = 0$, the odd-frequency component is absent. The gap equation becomes

$$\Delta = gT \sum_{\omega_n} \frac{1}{V_{\rm vol}} \sum_{\boldsymbol{k}} \frac{1}{2} {\rm Tr}[\mathcal{F}(\boldsymbol{k}, i\omega_n) i\hat{\sigma}_2]$$
$$= gN_0 \pi T \sum_{\omega_n} \frac{\Delta}{\sqrt{\omega_n^2 + \Delta^2}}, \tag{H8}$$

which is identical to that in the BCS theory, where N_0 is the density of states at the Fermi level per spin. It is possible to show that the superfluid density and the coefficients of the GL free energy are identical to those in the BCS theory,

$$Q_{\rm BCS} = 2n\pi T \sum_{\omega_n} \frac{\Delta^2}{(\omega_n^2 + \Delta^2)^{3/2}},$$
$$a_{\rm BCS} = \frac{1}{g} - N_0 \pi T \sum_{\omega_n} \frac{1}{|\omega_n|},$$
$$b_{\rm BCS} = \frac{N_0 \pi}{4} T \sum_{\omega_n} \frac{1}{|\omega_n|^3} = N_0 \frac{7\zeta(3)}{16(\pi T)^2}, \tag{H9}$$

where $\zeta(n)$ is Riemann zeta function. Therefore, the spin-orbit interactions do not change any thermal properties of a spin-singlet superconductor [1] as we discussed in the introduction.

Second, we consider the normal-state Hamiltonian including the Zeeman potential,

$$\hat{H}_{\rm N}(\boldsymbol{k}) = \xi_{\boldsymbol{k}} - \mu_{\rm B} \boldsymbol{B} \cdot \hat{\boldsymbol{\sigma}}, \tag{H10}$$

where $\mu_{\rm B}$ is Bohr's magneton and $\boldsymbol{B}$ is a Zeeman field. The odd-frequency pairing correlation appears because $P = 2\,\mu_{\rm B}\boldsymbol{B} \cdot \hat{\boldsymbol{\sigma}}$ remains finite. The Green's functions are calculated as

$$\mathcal{G}(\boldsymbol{k}, i\omega_n) = \frac{-1}{Z_z} \big[(i\omega_n + \xi_{\boldsymbol{k}})(\omega_n^2 + \xi_{\boldsymbol{k}}^2 + \Delta^2)$$
$$+ (i\omega_n - \xi_{\boldsymbol{k}})\mu_{\rm B}^2 B^2$$
$$+ \{(i\omega_n + \xi_{\boldsymbol{k}})^2 + \Delta^2 - \mu_{\rm B}^2 B^2\}\mu_{\rm B}\boldsymbol{B} \cdot \hat{\boldsymbol{\sigma}}\big], \tag{H11}$$

$$\mathcal{F}(\boldsymbol{k}, i\omega_n) = \frac{-1}{Z_z} \big[\omega_n^2 + \xi_{\boldsymbol{k}}^2 + \Delta^2 - \mu_{\rm B}^2 B^2 + 2i\omega_n \mu_{\rm B} \boldsymbol{B} \cdot \hat{\boldsymbol{\sigma}}\big] \Delta i\hat{\sigma}_2, \tag{H12}$$

$$Z_z = \xi_{\boldsymbol{k}}^4 + 2\xi_{\boldsymbol{k}}^2 A + C, \quad A = \Delta^2 + \omega_n^2 - \mu_{\rm B}^2 B^2,$$
$$C = A^2 + 4\omega_n^2 \mu_{\rm B}^2 B^2. \tag{H13}$$

The last term in $\mathcal{F}$ represents the pairing correlation belonging to odd-frequency spin-triplet s-wave symmetry class. The gap equation becomes

$$\Delta = gN_0 \pi T \sum_{\omega_n} \frac{\Delta\sqrt{A + \sqrt{C}}}{\sqrt{2C}}. \tag{H14}$$

The self-consistent pair potential $\Delta_{\rm eq}$ satisfies Eq. (H14) and minimizes the thermodynamic potential. The coefficients in the free energy result in

$$a = \frac{1}{g} - N_0 \pi T \sum_{\omega_n} \frac{\omega_n^2}{|\omega_n|(\omega_n^2 + \mu_{\rm B}^2 B^2)},$$
$$b = \frac{\sqrt{2}}{4} N_0 \pi T \sum_{\omega_n} \frac{A_0^3 + \sqrt{C_0}(A_0^2 - 2\omega_n^2 \mu_{\rm B}^2 B^2)}{[C_0(A_0 + \sqrt{C_0})]^{3/2}}, \tag{H15}$$

with $A_0 = A|_{\Delta=0}$ and $C_0 = C|_{\Delta=0}$. The second term of the coefficient a in Eq. (H15) becomes smaller than that in Eq. (H9), which leads to the suppression of T_c. The last term of the coefficient b in Eq. (H15) is derived from the odd-frequency pairing correlation function and decreases the coefficient b. The superfluid density is calculated to be

$$Q = 2\sqrt{2}n\pi T \sum_{\omega_n} \frac{\Delta^2\{A^3 + \sqrt{C}(A^2 - 2\omega_n^2\mu_B^2 B^2)\}}{[C(A+\sqrt{C})]^{3/2}}. \quad \text{(H16)}$$

The comparison between the expression of the superfluid density in Eq. (H16) and that of the coefficient b in Eq. (H15) shows that the odd-frequency pairing correlation decreases Q and b in exactly the same manner.

[1] P. A. Frigeri, D. F. Agterberg, A. Koga, and M. Sigrist, Superconductivity without inversion symmetry: MnSi versus $CePt_3Si$, Phys. Rev. Lett. **92**, 097001 (2004).

[2] G. Sarma, On the influence of a uniform exchange field acting on the spins of the conduction electrons in a superconductor, J. Phys. Chem. Solids **24**, 1029 (1963).

[3] K. Maki and T. Tsuneto, Pauli paramagnetism and superconducting state, Prog. Theor. Phys. **31**, 945 (1964).

[4] H. Menke, C. Timm, and P. M. R. Brydon, Bogoliubov Fermi surfaces stabilized by spin-orbit coupling, Phys. Rev. B **100**, 224505 (2019).

[5] A. Bianchi, R. Movshovich, N. Oeschler, P. Gegenwart, F. Steglich, J. D. Thompson, P. G. Pagliuso, and J. L. Sarrao, First-order superconducting phase transition in $CeCoIn_5$, Phys. Rev. Lett. **89**, 137002 (2002).

[6] H. A. Radovan, N. A. Fortune, T. P. Murphy, S. T. Hannahs, E. C. Palm, S. W. Tozer, and D. Hall, Magnetic enhancement of superconductivity from electron spin domains, Nature (London) **425**, 51 (2003).

[7] R. Lortz, Y. Wang, A. Demuer, P. H. M. Böttger, B. Bergk, G. Zwicknagl, Y. Nakazawa, and J. Wosnitza, Calorimetric evidence for a Fulde-Ferrell-Larkin-Ovchinnikov superconducting state in the layered organic superconductor κ-$(BEDT\text{-}TTF)_2Cu(NCS)_2$, Phys. Rev. Lett. **99**, 187002 (2007).

[8] V. L. Berezinskii, New model of the anisotropic phase of superfluid He^3, Pis'ma Zh. Eksp. Teor. Fiz. **20**, 628 (1974) [JETP Lett. **20**, 287 (1974)].

[9] F. S. Bergeret, A. F. Volkov, and K. B. Efetov, Odd triplet superconductivity and related phenomena in superconductor-ferromagnet structures, Rev. Mod. Phys. **77**, 1321 (2005).

[10] Y. Tanaka, M. Sato, and N. Nagaosa, Symmetry and topology in superconductors –odd-frequency pairing and edge states–, J. Phys. Soc. Jpn. **81**, 011013 (2012).

[11] J. Linder and A. V. Balatsky, Odd-frequency superconductivity, Rev. Mod. Phys. **91**, 045005 (2019).

[12] C. Triola, J. Cayao, and A. M. Black-Schaffer, The role of odd-frequency pairing in multiband superconductors, Ann. Phys. (Berlin, Ger.) **532**, 1900298 (2020).

[13] J. Cayao, C. Triola, and A. M. Black-Schaffer, Odd-frequency superconducting pairing in one-dimensional systems, Eur. Phys. J. Spec. Top. **229**, 545 (2020).

[14] Y. Tanuma, N. Hayashi, Y. Tanaka, and A. A. Golubov, Model for vortex-core tunneling spectroscopy of chiral p-wave superconductors via odd-frequency pairing states, Phys. Rev. Lett. **102**, 117003 (2009).

[15] D. Kuzmanovski, R. S. Souto, and A. V. Balatsky, Odd-frequency superconductivity near a magnetic impurity in a conventional superconductor, Phys. Rev. B **101**, 094505 (2020).

[16] V. Perrin, F. L. N. Santos, G. C. Ménard, C. Brun, T. Cren, M. Civelli, and P. Simon, Unveiling odd-frequency pairing around a magnetic impurity in a superconductor, Phys. Rev. Lett. **125**, 117003 (2020).

[17] Y. Tanaka and A. A. Golubov, Theory of the proximity effect in junctions with unconventional superconductors, Phys. Rev. Lett. **98**, 037003 (2007).

[18] Y. Asano and Y. Tanaka, Majorana fermions and odd-frequency Cooper pairs in a normal-metal nanowire proximity-coupled to a topological superconductor, Phys. Rev. B **87**, 104513 (2013).

[19] S.-I. Suzuki and Y. Asano, Paramagnetic instability of small topological superconductors, Phys. Rev. B **89**, 184508 (2014).

[20] S.-I. Suzuki, T. Sato, and Y. Asano, Odd-frequency Cooper pair around a magnetic impurity, Phys. Rev. B **106**, 104518 (2022).

[21] Y. Asano, A. A. Golubov, Y. V. Fominov, and Y. Tanaka, Unconventional surface impedance of a normal-metal film covering a spin-triplet superconductor due to odd-frequency Cooper pairs, Phys. Rev. Lett. **107**, 087001 (2011).

[22] A. M. Black-Schaffer and A. V. Balatsky, Odd-frequency superconducting pairing in multiband superconductors, Phys. Rev. B **88**, 104514 (2013).

[23] Y. Asano and A. Sasaki, Odd-frequency Cooper pairs in two-band superconductors and their magnetic response, Phys. Rev. B **92**, 224508 (2015).

[24] D. C. Cavanagh, D. F. Agterberg, and P. M. R. Brydon, Pair breaking in superconductors with strong spin-orbit coupling, Phys. Rev. B **107**, L060504 (2023).

[25] D. F. Agterberg, P. M. R. Brydon, and C. Timm, Bogoliubov fermi surfaces in superconductors with broken time-reversal symmetry, Phys. Rev. Lett. **118**, 127001 (2017).

[26] P. M. R. Brydon, D. F. Agterberg, H. Menke, and C. Timm, Bogoliubov Fermi surfaces: General theory, magnetic order, and topology, Phys. Rev. B **98**, 224509 (2018).

[27] J. M. Luttinger and W. Kohn, Motion of electrons and holes in perturbed periodic fields, Phys. Rev. **97**, 869 (1955).

[28] P. M. R. Brydon, L. Wang, M. Weinert, and D. F. Agterberg, Pairing of $j = 3/2$ fermions in half-Heusler superconductors, Phys. Rev. Lett. **116**, 177001 (2016).

[29] B. Roy, S. A. A. Ghorashi, M. S. Foster, and A. H. Nevidomskyy, Topological superconductivity of spin-3/2 carriers in a three-dimensional doped Luttinger semimetal, Phys. Rev. B **99**, 054505 (2019).

[30] G. Eilenberger, General approximation method for the free energy functional of superconducting alloys, Eur. Phys. J. A **190**, 142 (1966).

[31] H. G. Suh, H. Menke, P. M. R. Brydon, C. Timm, A. Ramires, and D. F. Agterberg, Stabilizing even-parity chiral superconductivity in Sr_2RuO_4, Phys. Rev. Res. **2**, 032023(R) (2020).

[32] D. Kim, S. Kobayashi, and Y. Asano, Josephson effect of superconductors with $J = \frac{3}{2}$ electrons, Phys. Rev. B **103**, 184516 (2021).
[33] D. Kim, T. Sato, S. Kobayashi, and Y. Asano, Spin susceptibility of a $J = 3/2$ superconductor, J. Phys. Soc. Jpn. **92**, 054703 (2023).
[34] A. Ramires and M. Sigrist, Identifying detrimental effects for multiorbital superconductivity: Application to Sr_2RuO_4, Phys. Rev. B **94**, 104501 (2016).
[35] A. Ramires, D. F. Agterberg, and M. Sigrist, Tailoring T_c by symmetry principles: The concept of superconducting fitness, Phys. Rev. B **98**, 024501 (2018).
[36] M. Sigrist and K. Ueda, Phenomenological theory of unconventional superconductivity, Rev. Mod. Phys. **63**, 239 (1991).
[37] M. Tinkham, *Introduction to Superconductivity* (McGraw-Hill, New York, 1996).
[38] A. Sasaki, S. Ikegaya, T. Habe, A. A. Golubov, and Y. Asano, Josephson effect in two-band superconductors, Phys. Rev. B **101**, 184501 (2020).
[39] A. Bhattacharya and C. Timm, Stability of Bogoliubov fermi surfaces within BCS theory, Phys. Rev. B **107**, L220501 (2023).
[40] M. Gomes da Silva, F. Dinóla Neto, I. Padilha, J. Ricardo de Sousa, and M. Continentino, First-order superconducting transition in the inter-band model, Phys. Lett. A **378**, 1396 (2014).
[41] B. S. Chandrasekhar, A note on the maximum critical field of high-field superconductors, Appl. Phys. Lett. **1**, 7 (1962).
[42] A. M. Clogston, Upper limit for the critical field in hard superconductors, Phys. Rev. Lett. **9**, 266 (1962).
[43] P. Fulde and R. A. Ferrell, Superconductivity in a strong spin-exchange field, Phys. Rev. **135**, A550 (1964).
[44] A. I. Larkin and Y. N. Ovchinnikov, Nonuniform state of superconductors, Zh. Eksp. Teor. Fiz. **47**, 1136 (1964) [Sov. Phys. JETP **20**, 762 (1965)].
[45] Y. Matsuda and H. Shimahara, Fulde-Ferrell-Larkin-Ovchinnikov state in heavy fermion superconductors, J. Phys. Soc. Jpn. **76**, 051005 (2007).
[46] H. Burkhardt and D. Rainer, Fulde-Ferrell-Larkin-Ovchinnikov state in layered superconductors, Ann. Phys. (Berlin, Ger.) **506**, 181 (1994).
[47] S. Matsuo, S. Higashitani, Y. Nagato, and K. Nagai, Phase diagram of the Fulde-Ferrell-Larkin-Ovchinnikov state in a three-dimensional superconductor, J. Phys. Soc. Jpn. **67**, 280 (1998).
[48] D. Chakraborty and A. M. Black-Schaffer, Interplay of finite-energy and finite-momentum superconducting pairing, Phys. Rev. B **106**, 024511 (2022).
[49] S.-I. Suzuki, T. Sato, A. A. Golubov, and Y. Asano, Fulde-Ferrell-Larkin-Ovchinnikov state in a superconducting thin film attached to a ferromagnetic cluster, Phys. Rev. B **108**, 064509 (2023).
[50] J. Schmidt, F. Parhizgar, and A. M. Black-Schaffer, Odd-frequency superconductivity and Meissner effect in the doped topological insulator Bi_2Se_3, Phys. Rev. B **101**, 180512(R) (2020).
[51] F. Parhizgar and A. M. Black-Schaffer, Diamagnetic and paramagnetic Meissner effect from odd-frequency pairing in multiorbital superconductors, Phys. Rev. B **104**, 054507 (2021).
[52] R. Peierls, Zur theorie des diamagnetismus von leitungselektronen, Eur. Phys. J. A **80**, 763 (1933).
[53] J. M. Luttinger, The effect of a magnetic field on electrons in a periodic potential, Phys. Rev. **84**, 814 (1951).
[54] D. J. Scalapino, S. R. White, and S. C. Zhang, Superfluid density and the Drude weight of the Hubbard model, Phys. Rev. Lett. **68**, 2830 (1992).
[55] D. J. Scalapino, S. R. White, and S. Zhang, Insulator, metal, or superconductor: The criteria, Phys. Rev. B **47**, 7995 (1993).
[56] T. Kostyrko, R. Micnas, and K. A. Chao, Gauge-invariant theory of the Meissner effect in the lattice model of a superconductor with local pairing, Phys. Rev. B **49**, 6158 (1994).
[57] A. A. Abrikosov, L. P. Gor'kov, and I. E. Dzyaloshinski, *Methods of Quantum Field Theory in Statistical Physics* (Dover Publications, New York, 1975).